

UNCLASSIFIED

AD 273 037

*Reproduced
by the*

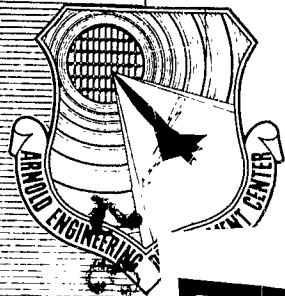
ARMED SERVICES TECHNICAL INFORMATION AGENCY
ARLINGTON HALL STATION
ARLINGTON 12, VIRGINIA



UNCLASSIFIED

NOTICE: When government or other drawings, specifications or other data are used for any purpose other than in connection with a definitely related government procurement operation, the U. S. Government thereby incurs no responsibility, nor any obligation whatsoever; and the fact that the Government may have formulated, furnished, or in any way supplied the said drawings, specifications, or other data is not to be regarded by implication or otherwise as in any manner licensing the holder or any other person or corporation, or conveying any rights or permission to manufacture, use or sell any patented invention that may in any way be related thereto.

AEDC-TDR-62-50



CATALOGED BY ASIA
AS AD NO. 273037

273 037

**FURTHER DEVELOPMENT
OF CAPACITANCE- AND INDUCTANCE-DRIVEN
HOTSHOT TUNNELS**

By

62-2-5

J. A. van der Blik
von Kármán Gas Dynamics Facility
ARO, Inc.

TECHNICAL DOCUMENTARY REPORT NO. AEDC-TDR-62-50

March 1962

AFSC Program Area 750A, Project 8952, Task 89512

(Prepared under Contract No. AF 40(600)-800 S/A 24(61-73) by ARO, Inc.,
contract operator of AEDC, Arnold Air Force Station, Tennessee)

**ARNOLD ENGINEERING DEVELOPMENT CENTER
AIR FORCE SYSTEMS COMMAND
UNITED STATES AIR FORCE**

FURTHER DEVELOPMENT
OF CAPACITANCE- AND INDUCTANCE-DRIVEN
HOTSHOT TUNNELS*

By

J. A. van der Blik

von Kármán Gas Dynamics Facility

ARO, Inc. ,

a subsidiary of Sverdrup and Parcel, Inc.

March 1962

ARO Project Nos. 360212 and 360213

*Paper presented at the Second National Symposium on Hyper-velocity Techniques, March 19-20, 1962, University of Denver, Denver, Colorado.

ABSTRACT

Significant developments of the hotshot tunnels in the von Kármán Gas Dynamics Facility, Arnold Engineering Development Center, Arnold Air Force Station, Tennessee, since the First National Symposium on Hypervelocity Techniques are described.

An arc chamber with coaxial electrodes was developed for the inductance-driven 50-Inch Hypervelocity Tunnel (Hotshot 2). Combined with a short-circuit switch, to reduce the discharge time, this configuration resulted in a significant decrease in flow contamination. Force tests in the Mach number range from 16-22 at stagnation temperatures from 3000-4000°K and stagnation pressures from 10,000-20,000 psi were in good agreement with results from other tunnels.

An arc-chamber liner material study was carried out in the capacitance-driven Tunnel Hotshot 1. The materials tested included copper, boron nitride, graphite, tungsten, and chrome-plated copper.

The heat losses through the arc-chamber walls of Hotshot 1, determined from runs at stagnation temperatures from 3000-9000°K, are presented, and their implications on hotshot tunnel operation are discussed.

CONTENTS

	<u>Page</u>
ABSTRACT.	iii
NOMENCLATURE.	vii
1.0 INTRODUCTION	1
2.0 DESCRIPTION OF HYPERVELOCITY (HOTSHOT) TUNNELS.	1
3.0 ARC-CHAMBER DEVELOPMENT, 50-INCH HYPERVELOCITY TUNNEL	3
4.0 EXPERIMENTAL RESULTS, 50-INCH HYPER- VELOCITY TUNNEL	4
5.0 LINER DEVELOPMENT, HOTSHOT 1	5
6.0 EXPERIMENTAL RESULTS, HOTSHOT 1.	5
7.0 COMPARISON OF MATERIAL PROPERTIES	6
8.0 HEAT LOSS THROUGH THE ARC-CHAMBER WALL	7
9.0 TEMPERATURE DECAY ESTIMATES FOR HIGH TEMPERATURES	10
10.0 CONCLUSIONS	11
REFERENCES	12

ILLUSTRATIONS

Figure

1. Tunnel Hotshot 1, a 16-in. -diam Hypervelocity Wind Tunnel	15
2. The 50-Inch Hypervelocity Wind Tunnel (Tunnel Hotshot 2).	16
3. The 100-Inch Hypervelocity Wind Tunnel (Tunnel F).	17
4. Typical Oscillograph Traces and Timewise Variation of C_D and \dot{q} in the 50-Inch Hypervelocity Tunnel (Hotshot 2).	18
5. Schematic of Inductance Energy Storage System of the 50-Inch Hypervelocity Tunnel (Hotshot 2).	19
6. Typical Current and Voltage Traces without and with Short Circuit Switch (Hotshot 2).	20
7. Coaxial Arc Chambers of the 50-Inch Hypervelocity Tunnel (Hotshot 2).	21

<u>Figure</u>	<u>Page</u>
8. Summary of Test Results Obtained with Various Arc Chambers in the 50-Inch Hypervelocity Tunnel (Hotshot 2)	22
9. Drag Coefficients from Two Blunt 9-deg Cones, Nose to Base Radius Ratio of 0.3, Base Radii of 1-in. and 3-in. (Hotshot 2)	23
10. Arc Chamber 16-C of the 16-in. -diam Hypervelocity Tunnel, Hotshot 1	24
11. Summary of Test Results with Various Arc-Chamber Liner Materials in Tunnel Hotshot 1.	25
12. Temperature Decay in the 16-C Chamber (Hotshot 1)	26
13. Temperature Rise in Semi-Infinite Solid and Infinite Hollow Cylinder	26
14. Temperature Rise in Infinite Slab on Insulator	27
15. Temperature Rise in Semi-Infinite Wall for Different Materials	27
16. Comparison of Liner Materials	28
17. Experimental Arc-Chamber Heat Loss in Tunnel Hotshot 1.	29
18. Experimental Arc-Chamber Heat Loss in the 50-Inch Hypervelocity Tunnel (Hotshot 2)	30
19. Experimental Enthalpy Decay with Various Liner Materials (Hotshot 1)	31
20. Experimental Enthalpy Decay for Three Different Densities (Hotshot 2)	32
21. Experimental Enthalpy Decay with Helium (Hotshot 1)	32
22. Internal Energy for Air and Nitrogen	33
23. Enthalpy and Maximum Velocity for Air	34
24. Temperature Decay Caused by Radiation for Air in Closed Reservoir	35
25. Required Energy for Desired Air Temperature at Time of Test.	36

NOMENCLATURE

A	Arc-chamber surface area, ft ²
A*	Throat area, ft ²
a	Speed of sound, ft/sec
C _D	Drag coefficient
C _v	Specific heat of gas at constant volume, ft ² /sec ² °K
c	Specific heat of solid, ft ² /sec ² °K
D	Arc-chamber diameter, ft
d*	Throat diameter, ft
E	Internal energy per volume, lb/ft ²
e	Specific internal energy, ft ² /sec ²
h	Specific enthalpy, ft ² /sec ²
L	Arc-chamber length, ft
l	Slab thickness, cf Fig. 14
M	Mach number
p	Pressure, lb/ft ²
Q	Heat input per unit volume, lb/ft ²
q̇	Heat transfer rate, Btu/ft ² sec
R	Gas constant, ft ² /sec ² °K
Re	Reynolds number
T	Temperature, °K
t	Time, sec
u	Velocity, ft/sec
V	Arc-chamber volume, ft ³
W	Work per unit volume, lb/ft ²
α	=λ/ρc thermal diffusivity, ft ² /sec
γ	Ratio of specific heats for gas
λ	Thermal conductivity, Btu/ft-sec °K
ρ	Density, lb sec ² /ft ⁴ , or amagat = density relative to gas at room temperature and pressure

σ Stefan-Boltzmann constant = 5×10^{-12} Btu/ft²sec (°K)⁴
 τ Dimensionless time parameter

SUBSCRIPTS

o Stagnation (reservoir) condition
i Initial condition, $t = 0$
 ∞ Free-stream condition

SUPERSCRIPTS

1 Stagnation condition behind normal shock
* Sonic throat condition

1.0 INTRODUCTION

This report deals with development of the hotshot tunnels in the von Kármán Gas Dynamics Facility (VKF) at the Arnold Engineering Development Center, Air Force Systems Command, USAF, since the First National Symposium on Hypervelocity Techniques (Ref. 1). The major obstacle in carrying out useful aerodynamic measurements in hotshot tunnels appeared to be contamination of the flow with solid particles eroded from the electrodes and arc-chamber walls. The improvements in arc-chamber design, described in Ref. 1, led to a coaxial electrode configuration for the capacitance-driven Tunnel Hotshot 1 with which satisfactory force and pressure tests could be carried out at moderately high stagnation temperatures (3000-4000°K) and relatively high stagnation densities (50-150 amagat).

A coaxial arc chamber was developed for the inductance-driven 50-Inch Hypervelocity Tunnel (Tunnel Hotshot 2) (Ref. 2). During the past 18 months the coaxial configurations have been used for a large number of ballistic missile and re-entry configuration tests, and also an internal research program on viscous interaction effects was begun (see Refs. 3 and 4). The usefulness of these tests lies in the correct Mach number and Reynolds number simulation.

A series of exploratory tests at higher arc-chamber temperatures were carried out in the capacitance-driven Tunnel Hotshot 1 (Ref. 5). These tests provided data on materials at temperatures from 5000 to 10,000°K and data on the heat loss through the arc-chamber wall.

2.0 DESCRIPTION OF HYPERVELOCITY (HOTSHOT) TUNNELS

The von Kármán Gas Dynamics Facility has three hotshot-type tunnels with test section diameters of 16, 50, and 100 inches, respectively (Figs. 1, 2, and 3). The first is driven by a capacitor bank of one megajoule, whereas the last two are driven by inductance power supplies of ten and one hundred megajoule capacities, respectively. The 100-inch tunnel is now being prepared for operation.

The tunnels consist of an arc chamber (reservoir), conical nozzle, and test section followed by a cylindrical vacuum tank. The main dimensions of the tunnels are summarized in the following table.

Manuscript released by author February 1962.

Tunnel	Hotshot 1	50-In. Hypervelocity Tunnel (Hotshot 2)		100-In. Hypervelocity Tunnel (Tunnel F)
<u>Arc Chambers</u>				
designation	16-C	50-M	50-O	100-A
length, L, in.	6.5	16	10	14
diameter, D, in.	2.5	5	6.3	13
volume, V, in. ³	30	350	350	1860
<u>Nozzles, Conical</u>				
included angle, deg	10	10		8
length, in.	91	285		775
<u>Test Section</u>				
diameter, in.	16	50		108
length, in.	36	72		---
shape	cylindrical	cylindrical		conical
<u>Vacuum Tank</u>				
diameter, ft	2	6		9.7
length, ft	12	35		57
volume, ft ³	38	957		4240
<u>Energy Storage</u>				
type	capacitance	inductance		inductance
max. energy, megajoule	1 at 4000 V, C = 1/8 farad	10 at 245,000 amp, L = 350 henry		100 at 1,000,000 amp, L = 200 henry

Before a tunnel run the nozzle, test section, and vacuum tank are evacuated to a pressure of one to ten microns Hg. The arc chamber is initially charged with the test gas to a pressure of 50-150 atm at room temperature. With the exception of a few air and helium runs, the data here reported were obtained with nitrogen. Electrical energy is discharged in an arc struck between the electrodes in the arc chamber. The resulting pressure and temperature rise of the arc-chamber gas causes rupture of the diaphragm, located between the arc chamber and nozzle. After a starting process, quasi-steady hypersonic flow is established in the nozzle and test section for a period of 20 to 100 milliseconds. A typical run trace and timewise reduced data of the 50-Inch Hypervelocity Tunnel (Hotshot 2) are shown in Fig. 4.

The operation of the tunnels is fully described in Ref. 1, whereas details on tunnel instrumentation and data reduction are given in Refs. 6 and 7.

Since the writing of Ref. 1, no changes have been made in the capacitance system of Hotshot 1.

A schematic drawing of the inductance energy storage system of the 50-Inch Hypervelocity Tunnel (Hotshot 2) is given in Fig. 5. The arrangement in Fig. 5a is identical to that of Ref. 1 except for the short circuit switch. The short circuit switch was installed when the coaxial arc chamber 50-M was in use (Ref. 2). It reduces the arc duration to 6-9 msec (Fig. 6).

As was noted in Ref. 1, the voltage limitation of this power supply was determined by the insulation between the generator, flywheel, and ground. By grounding one leg of the bus and the outer electrode (Fig. 5b) and by adding high voltage insulation the system is now insulated for 20,000 volts in contrast to the previous 7000-volt limit. These modifications were made when the new coaxial arc chamber, 50-O, was installed.

3.0 ARC-CHAMBER DEVELOPMENT, 50-INCH HYPERVELOCITY TUNNEL

The use of a coaxial electrode configuration in the Hotshot 1 arc chamber resulted in significant improvements (Ref. 1). Consequently, the parallel electrode configuration 50-D, in Hotshot 2, was replaced by a coaxial one. The development of the coaxial electrodes, described in Ref. 2, resulted in an improved arc chamber, 50-M (Fig. 7a), for the temperature range of $T_0 = 3000-4000^\circ\text{K}$ and $\rho_0 = 50-150$ amagat. Finally, a simplified design with a smaller length-to-diameter ratio was built and installed at the same time when the electrical bus modifications were carried out. The last configuration, 50-O, has the same volume as the 50-M arc chamber (- 350 cu in.) and the materials used are identical (Fig. 7b). As in the 16-C arc chamber of Hotshot 1, the Hotshot 2 arc chambers have an electrically integral liner and outer electrode (linertrode). Maintaining the electrode block and the outer electrode at the same potential as the surrounding gun breech block allowed considerable simplification at the electrode end of the chamber. Further simplification was achieved by adopting a preloaded nylon-wedge pressure seal system.

4.0 EXPERIMENTAL RESULTS, 50-INCH HYPERVELOCITY TUNNEL

The results obtained with the coaxial arc chambers 50-M and 50-O are summarized in Fig. 8. For comparison, results obtained with the first (50-A) and last (50-D) parallel electrode configurations are included.

The 50-M arc chamber (Fig. 7a) resulted in a total weight loss of 15 to 30 grams or 2 to 4 percent of the gas mass in the arc chamber for a 100-amagat run. With the 50-O arc chamber the total weight loss was again reduced by a factor of two and this is mainly caused by the liner-electrode (linertrode) which now has a net gain in weight.

The weight increase of a 3 x 1-inch slide, mounted 5 inches from the test section wall and perpendicular to the flow direction, was measured after each run. The progressive decrease in weight gain of this particle collector is in agreement with the reduction in total weight loss of the arc-chamber components (Fig. 8).

In Fig. 8, the stagnation point heat transfer coefficient measured on hemisphere-cylinder models is compared with the theory of Ref. 8, assuming a Lewis number equal to one. As in Ref. 1, the heat transfer measurements were improved as contamination was reduced. However, large timewise variations occurred during the useful part of many runs, and repeatability from run to run was poor. With the 50-M arc chamber the measurements scattered with a band of ± 30 percent of theory. Although this was a great improvement compared to results with earlier arc-chamber configurations, it is clear that the consistency of these measurements was not yet satisfactory.

A comparison of drag measurements carried out with the 50-M arc chamber on slender wing bodies was made in Ref. 2. Good agreement was obtained with data from Hotshot 1, the Boeing 44-inch hotshot tunnel, the AEDC 50-Inch Mach 8 Tunnel, and the 24-inch shock tunnel of the Cornell Aeronautical Laboratory.

The reduction in weight loss of the arc-chamber components by a factor of two with the 50-O chamber did not change the scatter of heat transfer rates measured in the test section (Fig. 8), which still fluctuated at least ± 30 percent around the theoretical value. Errors in measurement are estimated to be less than ± 10 percent.

Drag measurements carried out on 9-deg cone models are given in Fig. 9. Good agreement between the data with the 50-M and 50-O configurations was obtained.

5.0 LINER DEVELOPMENT, HOTSHOT 1

In an effort to extend the temperature range of the hotshot tunnels a series of tests was carried out with the 16-C coaxial arc chamber (Fig. 10) using various liner materials. The materials tested were: copper, chrome-plated copper, tungsten, boron nitride, and graphite. The tests were carried out with nitrogen except for some runs in which air was used. Since copper was a fairly satisfactory material in the temperature range of 3000-4000°K the use of other, and more expensive, materials would only be advantageous at higher temperatures, 5000-10,000°K, where copper liners produce a large amount of contamination. Simple particle theory (Ref. 1) indicates that tests with a larger throat diameter ($d^* = 0.15$ in. as compared with medium $d^* = 0.11$ in.) will produce a larger particle effect on aerodynamic measurements in the test section. Thus to bring out differences in particle contamination with various arc-chamber liner materials the tests were carried out at reservoir temperatures $T_0 \approx 6000-9000^\circ\text{K}$ and with a large throat diameter, $d^* = 0.15$ in. Also, for the same reason, a baffle was not used in most of the runs.

6.0 EXPERIMENTAL RESULTS, HOTSHOT 1

The copper liners were remachined and polished after every run. The surfaces of the tungsten, boron nitride, and graphite liners were cleaned and the rough spots removed after each run. The surfaces were given a finish comparable to new liners.

Because of the tendency of ceramic-type materials to crack, the boron nitride and graphite liners were split longitudinally into four equal segments. The life of the boron nitride liner was eight shots. The graphite liner was serviceable after ten shots.

Three types of tungsten were tried. A 0.017-inch tungsten sheet was rolled into a cylinder, then silver-soldered to the arc chamber. This configuration was unsatisfactory; the tungsten sheet shattered on the first shot. A plasma-sprayed, tungsten liner was also unsatisfactory because it cracked during the first shot and spalled extensively during the second shot. A pressed-sintered, tungsten liner cracked during the first shot, but was still serviceable after thirty shots.

Two copper liners were plated with chromium about 0.001-inch thick. The chromium in the vicinity of the arc disappeared upon firing.

The stagnation point heat rates, measured on a one-inch-diameter hemisphere, and the arc-chamber weight losses are summarized in Fig. 11. With copper liners, small throat ($d^* = 0.11$ in.), baffle plate in, and at $T_0 = 3500^\circ\text{K}$ the heat rates are about the same as in Hotshot 2, ± 30 percent deviation from theory. The baffle plate has a marked effect at these conditions. With a large throat ($d^* = 0.15$ in.) the measured heat rates become considerably higher, up to 85 percent above theory without baffle plate. The arc-chamber weight loss varied between 2 and 6 percent of the gas mass. Nitrogen runs at 6000 and 9000 $^\circ\text{K}$ showed a progressive increase in relative heat transfer rate. The 6000 $^\circ\text{K}$ air runs gave heat transfer rates about three times higher than the nitrogen runs with the same throat size. Some improvement with a small throat and baffle plate may be expected at temperatures from 6000 to 9000 $^\circ\text{K}$.

With tungsten liners a pattern similar to that obtained with copper liners is shown in Fig. 11. Tungsten appears to be more promising than copper with nitrogen at high temperature. The 6000 $^\circ\text{K}$ air runs with tungsten liners also produced lower heat rates than with copper liners.

Boron nitride and graphite liners at 6000 $^\circ\text{K}$ gave about the same results as tungsten. The total arc-chamber weight loss for the temperature range of 6000-9000 $^\circ\text{K}$ was excessive for all configurations tested.

The temperature of the gas in the arc chamber is given as a function of time after diaphragm break in Fig. 12. Since the useful run time in Hotshot 1 usually occurs from 15 to 25 milliseconds after the diaphragm breaks, the seriousness of the decay with increasing temperature is apparent. This problem is further discussed in Section 9.

7.0 COMPARISON OF MATERIAL PROPERTIES

It is desirable that the temperature of the arc-chamber wall material does not exceed the melting or sublimation point during the useful part of the tunnel run. A reasonable basis for comparing liner materials is the wall temperature rise for constant heat input.

Comparison of the wall temperature rise (Ref. 11) of a semi-infinite solid and an infinite hollow cylinder (Fig. 13) shows that for the largest value of the dimensionless time parameter, τ , under consideration ($\tau = 0.012$ for $t = 0.10$ sec with copper liner for Hotshot 1), the semi-infinite wall case is a good approximation. The effect of liner thickness on the internal wall temperature can be judged by comparing the temperature rise of the back and front of a slab mounted on a thermal

insulator (Ref. 11). For $\tau = 0.2$ the back temperature rise can be neglected (Fig. 14). For the most unfavorable case under consideration, a copper liner of 0.25-in. thickness, $\tau = 0.2$ gives $t = 0.070$ sec.

The wall temperature rise for a semi-infinite solid was calculated for various materials (Fig. 15) for a constant heat rate input of 10,000 Btu/ft²sec, which is representative for runs with reservoir temperatures of 6000-9000°K. The relatively low copper and tungsten temperatures are apparent. The time required to reach the melting or sublimation point for various materials, assuming a constant heat input rate and a semi-infinite wall, is given in Fig. 16a. The scale is relative to tungsten. Tungsten is far better than any other material. It also appears from Fig. 16a that some materials with a high melting point, such as tantalum, boron nitride, and platinum, are not better than copper, which itself has a melting time of only 30 percent that of tungsten. Ceramic materials have, in general, a low thermal conductivity and fall in the category of 20 percent or less of the tungsten melting time. Ceramic materials also have poor mechanical resistance against thermal shock.

When operating with air, the problem of accelerated oxidation or ignition (Ref. 12) becomes important, and its significance was pointed out in Ref. 1 in connection with throat erosion. The estimated times to reach ignition temperatures (or melting temperature when the material melts before it ignites) are given in Fig. 16b for the same materials as in Fig. 16a. The scale used is the same as in Fig. 16a. Copper, which melts before it ignites, is now the best material in this group. Beryllium does not seem to offer any advantages over copper, particularly since erosion and machining of beryllium introduce health hazards.

From this comparison it would be expected that tungsten is the best material for nitrogen and copper the best material for tests with air. The large amount of contamination in the Hotshot 1 tests precludes a definite conclusion at this time, although tungsten appeared to be better in both cases.

8.0 HEAT LOSS THROUGH THE ARC-CHAMBER WALL

The decay of arc-chamber pressure and temperature with time is caused by the mass flow through the throat and the heat loss through the arc-chamber wall. The first law of thermodynamics gives per unit volume:

$$dQ = dE + dW$$

Hence

$$dQ = \rho_o V de_o + p_o dV = - \dot{q} A dt$$

and

$$- \dot{q} \frac{A}{V} = \rho_o \frac{de_o}{dt} - \frac{p_o}{\rho_o} \frac{d\rho_o}{dt} \quad (1)$$

where \dot{q} is the average heat lost per unit time and per unit area over the arc-chamber area, A . With the definition of specific enthalpy:

$$h_o = e_o + \frac{p_o}{\rho_o}$$

and the mass flow equation:

$$V \frac{d\rho_o}{dt} = - \rho^* u^* A^*$$

the heat loss rate becomes:

$$\left. \begin{aligned} \dot{q} &= - \left[\frac{d(\rho_o e_o)}{dt} \frac{V}{A} + h_o \rho^* u^* \frac{A^*}{A} \right] \\ \text{or} \quad \dot{q} &= - \frac{V}{A} \left[\frac{d(\rho_o e_o)}{dt} - h_o \frac{d\rho_o}{dt} \right] \end{aligned} \right\} \quad (2)$$

The quantities ρ_o , e_o , and h_o are obtained as a function of time with the normal data reduction program (Ref. 7). For a number of runs in Hotshot 1 and Hotshot 2, the average heat rate, \dot{q} , was determined with Eq. (2). The results for the 16-C and 50-M arc chambers with copper liners are plotted as a function of temperature in Figs. 17 and 18, respectively. Each of the shaded areas covers a number of runs with approximately the same initial temperature and density. The shaded areas in Figs. 17 and 18 include the timewise variation during a run. As far as black-body radiation is concerned, the wall temperature increase during a run (see Section 7) has little influence.

For temperatures above 6000°K and gas densities greater than 10 amagat the total emissivity of the gas volume for the present arc chambers is expected to be equal to one, based on air data given in Ref. 14, so that the gas volume radiates as a black body. Except for the 9000°K, 15-amagat runs (Fig. 17), the experimental heat transfer rate is greater than black-body radiation.

At lower temperatures and higher densities the heat transfer process appears to be dominated by convection and conduction, whereas at higher temperatures the process is dominated by black-body radiation.

The main conclusion from Fig. 17 is that for $T_o > 6000^\circ\text{K}$ and $\rho_o > 20$ amagat the heat loss amounts to at least black-body radiation, as would

be expected. At present there are not enough accurate data to correlate the convection and conduction heat losses in a consistent manner. Fortunately, at lower temperatures where the latter dominate, the heat loss through the arc-chamber wall does not constitute a major problem.

The enthalpy decay obtained with five different arc-chamber materials in Hotshot 1 is given in Fig. 19. On the basis of Fig. 15 the order of materials giving increasing heat loss would be: copper, tungsten, graphite, and boron nitride. The experimental data in Fig. 19 show that the wall material has a small influence on the enthalpy decay.

The relative importance of mass flow effects on temperature decay can be illustrated by considering a perfect gas, $Z = 1$, $\gamma = \text{constant}$, with radiation loss only. Equation (2) then becomes

$$\sigma \frac{A}{V} T_o^4 + C_v \rho_o \frac{dT_o}{dt} + RK \frac{A^*}{V} \rho_o a_o T_o = 0$$

where $K = K(\gamma) = \left(\frac{2}{\gamma + 1} \right)^{\frac{1}{2} \frac{\gamma + 1}{\gamma - 1}}$, for $\gamma = 1.4$: $K = 0.578$.

The rate of temperature decay is

$$-\frac{dT_o}{dt} = \frac{\sigma}{C_v} \frac{A}{V} \frac{T_o^4}{\rho_o} + \frac{RK\sqrt{\gamma R}}{C_v} \frac{A^*}{V} T_o^{3/2} \quad (3)$$

and so

$$\beta = \frac{(\Delta T)_{\text{heat loss}}}{(\Delta T)_{\text{mass flow}}} = \frac{\sigma}{R^{3/2} \sqrt{\gamma K}} \frac{A}{A^*} \frac{T_o^{5/2}}{\rho_o} \quad (4)$$

It is clear from Eq. (4) that at higher temperatures and lower densities the effect of mass flow through the throat on arc-chamber temperature becomes very small.

Experimental results obtained in Hotshot 2 illustrate the density effect on enthalpy decay (see Fig. 20).

The experimental heat loss results presented so far were all obtained with nitrogen. When using helium, a light gas with low value of $C_v \rho_o$, at a given temperature, the decay is much larger even at low temperature (Fig. 21). The heat losses through the arc-chamber wall were in substantial agreement with those obtained with nitrogen.

9.0 TEMPERATURE DECAY ESTIMATES FOR HIGH TEMPERATURES

Neglecting mass flow effects and assuming black-body radiation, Eq. (1) becomes

$$\frac{At}{V} = \frac{\rho_o}{\sigma} \int_{T_o}^{T_{oi}} \frac{de_o}{T_o^4} \quad (5)$$

The specific internal energy of air and nitrogen is given as a function of temperature for various densities in Fig. 22. The enthalpy and maximum velocity, $u_{\max} = \sqrt{2h_o}$, for air are given as a function of temperature in Fig. 23.

Using Eq. (5) and integrating numerically, the temperature decay was calculated, for air at different densities, as a function of At/V (Fig. 24) for initial temperatures between 8000 and 16,000°K. Two trends are immediately apparent:

1. Over the density range considered, the temperature is practically independent of the initial value T_{oi} for $At/V > 1$ and,
2. for a given initial temperature T_{oi} , the temperature at a given At/V is strongly dependent on density.

In order to relate these estimates to present operational conditions of VKF hotshot tunnels, the table below has been prepared. The values of t_1 listed are the earliest times at which aerodynamic data can be taken following initiation of the arc discharge.

Tunnel	Test Section Diam, in.	A/V , ft^{-1}	t_1 , msec	At_1/V , sec/ft
Tunnel Hotshot 1	16	24.0	20	0.48
50-Inch Hypervelocity Tunnel	50	10.0	40	0.40
100-Inch Hypervelocity Tunnel	100	5.4	(70)	(0.38)

() - Estimated Value

Assuming that the useful test time is equal to t_1 , it is evident that present hotshot operation corresponds to At/V values from about 0.4 to 1. Inspection of Fig. 24 indicates that operation between these limits at high

temperatures may be only possible at high densities and that test temperatures exceeding 10,000°K would be, in general, difficult to reach. For example, at $\rho_0 = 100$ amagat and $At/V = 0.7$ an initial temperature of 16,000°K and a density of 100 amagat are necessary to obtain a temperature of 10,000°K, even neglecting conduction and convection heat losses, which would be appreciable at the high density.

The analysis here presented is generally applicable to any aerodynamic test facility which employs reservoir heating. The severity of the problem of heat losses was pointed out in Ref. 15 in connection with the performance of reflected shock tunnels. Nevertheless, the attainment of high temperatures in shock tunnels, which operate at times an order of magnitude smaller than the present hotshot tunnels, should be much easier in this respect.

The initial energy per unit volume, required in the gas to obtain a given temperature at various values of At/V , is plotted in Fig. 25. Also listed in this figure are the available energies per unit arc-chamber volume for the present AEDC hypervelocity tunnels. The 100-Inch Hypervelocity Tunnel with 93 megajoule/ft³ probably cannot deliver more than 60 megajoule/ft³ to the gas, which means that the maximum temperatures attainable with 40 and 100 amagat at $At/V = 0.4$ are 9000 and 8200°K, respectively, with initial temperatures of 15,000 and 10,000°K.

The value of A/V is relatively insensitive to the shape of the arc chamber and depends mainly on the size (volume). Reduction of time between diaphragm break and time when aerodynamic data are taken would require shorter tunnel starting times and faster response instrumentation than is now being used in the VKF hotshot tunnels.

10.0 CONCLUSIONS

The present status of the VKF hypervelocity tunnels can be summarized as follows:

Arc-chamber and circuit development of the inductance-driven 50-Inch Hypervelocity Tunnel (Hotshot 2) have resulted in a facility of quality equal to that of the capacitance-driven Tunnel Hotshot 1.

In the moderately high temperature range of 3000-4000°K at reservoir densities of 50-150 amagat, reliable aerodynamic data (pressure and force tests) are obtained, both in the capacitance- and inductance-driven tunnels. In this regime Mach number and Reynolds number

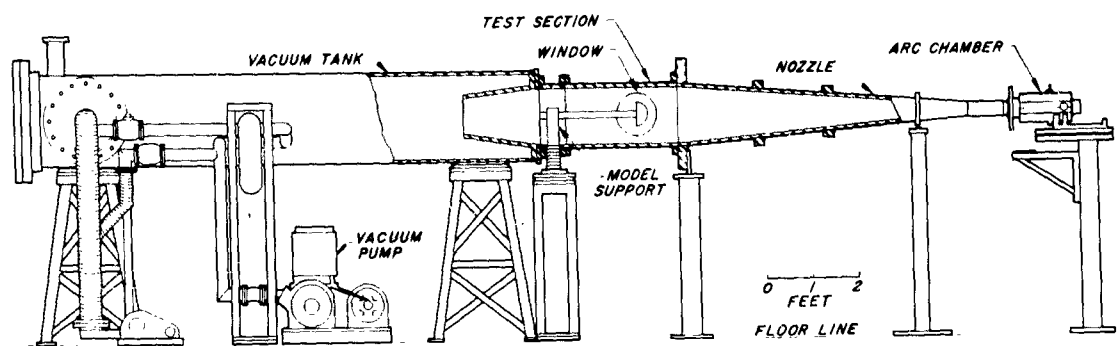
simulation is obtained for re-entry trajectories. The consistency of heat transfer measurements is still unsatisfactory.

Velocity simulation for re-entry trajectories ($T_0 = 10,000^\circ\text{K}$) introduces problems of arc-chamber materials and heat losses. Operation at shorter times and higher reservoir densities would tend to alleviate these problems.

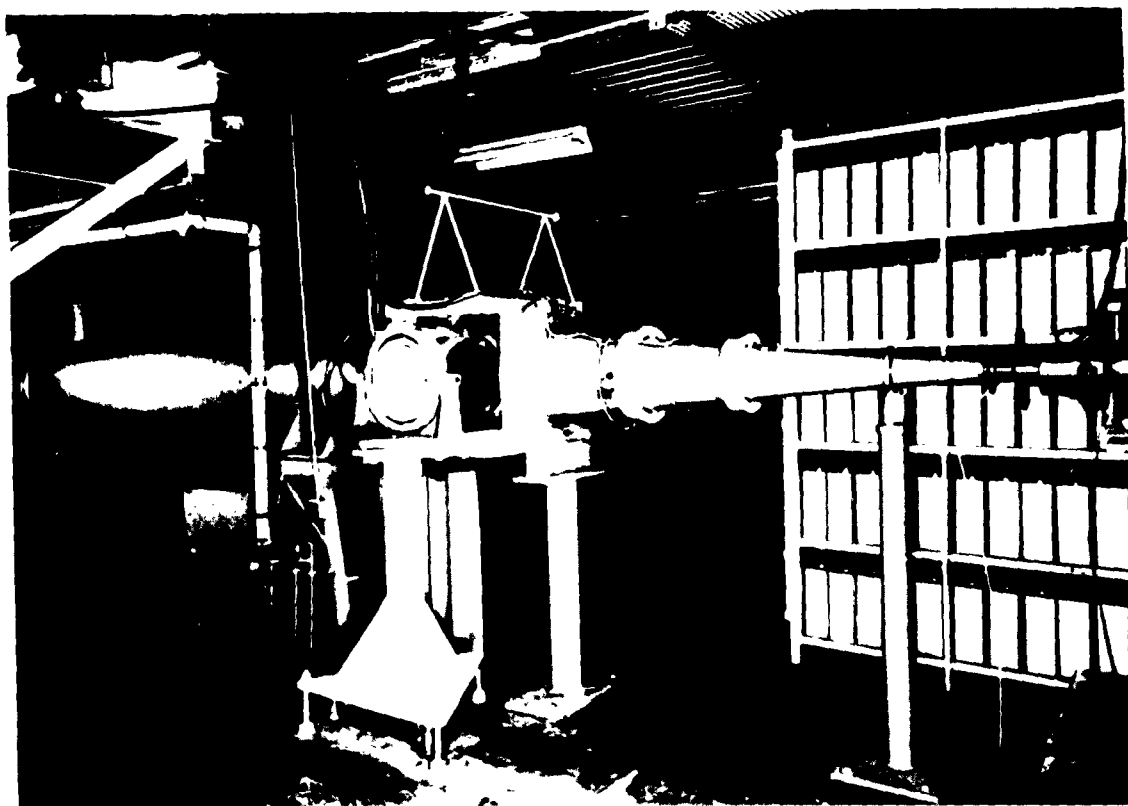
REFERENCES

1. Lukasiewicz, J., Harris, W. G., Jackson, R., van der Blik, J. A., and Miller, R. M. "Development of Capacitance and Inductance Driven Hotshot Tunnels." AEDC-TN-60-222, January 1961, and Proceedings National Symposium on Hypervelocity Techniques, October 1960, Denver, Colorado. IAS Publication.
2. van der Blik, J. A., Desjins, H. E., and Walker, R. R., III. "Further Development of an Inductance-Driven Hotshot Tunnel." AEDC-TN-61-80, July 1961.
3. Lukasiewicz, J., Whitfield, J. D., and Jackson, R. "Aerodynamic Testing at Mach Numbers from 15 to 20." International Hypersonics Conference, August 1961, Cambridge, Massachusetts. ARS Preprint 1969-61.
4. Lewis, C. H. "Pressure Distribution and Shock Shape over Blunted Slender Cones at Mach Numbers from 16 to 19." AEDC-TN-61-81, August 1961.
5. Smithson, H. K. "Arc-Chamber Liner Material Experiments in a Capacitance-Driven Hotshot Tunnel." AEDC-TDR (to be published).
6. Earheart, W. T., Jr. and Bynum, D. S. "Hypervelocity Arc-Tunnel Instrumentation." AEDC-TN-60-227, December 1960.
7. Grabau, M., Humphrey, R. L., and Little, W. J. "Determination of Test-Section, after Shock and Stagnation Conditions in Hotshot Tunnels Using Real Nitrogen at Temperatures from 3000 to 4000°K." AEDC-TN-61-82, July 1961.
8. Fay, J. A. and Riddell, F. R. "Theory of Stagnation Point Heat Transfer in Dissociating Air." Journal of the Aeronautical Sciences, February 1958, pp. 73-85.

9. Humphrey, R. L., Little, W. J., and Seeley, L. A. "Mollier Diagram for Nitrogen." AEDC-TN-60-83, May 1960.
10. Hilsenrath, J., Klein, M., and Woolley, H. W. "Tables of Thermodynamic Properties of Air Including Dissociation and Ionization from 1500 to 15,000°K." AEDC-TR-59-20, December 1959.
11. Carslaw, H. S. and Jaeger, J. C. Conduction of Heat in Solids. Oxford University Press, 1959. (Second Edition).
12. Reynolds, W. C. "Investigation of Ignition Temperatures of Solid Metals." NASA TN D-182, October 1959.
13. Bro, P. and Steinberg, S. "Surface Behavior of Boron Nitride in High Temperature Arc Heated Gases." American Rocket Society Journal, October 1961, pp. 1460-1462.
14. Kivel, B. "Radiation from Hot Air and Stagnation Heating." AVCO Research Report 79, October 1959.
15. Wittliff, C. E., Wilson, M. R., and Herzberg, A. "The Tailored-Interface Hypersonic Shock Tunnel." Journal of the Aero/Space Sciences, April 1959, pp. 219-228.

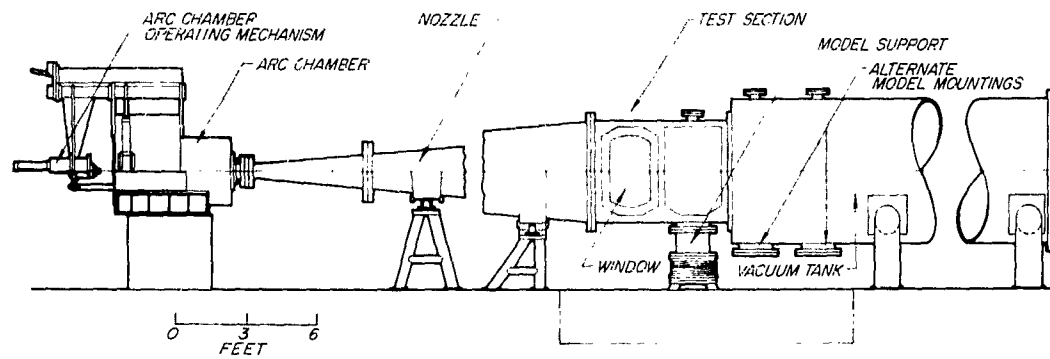


Assembly

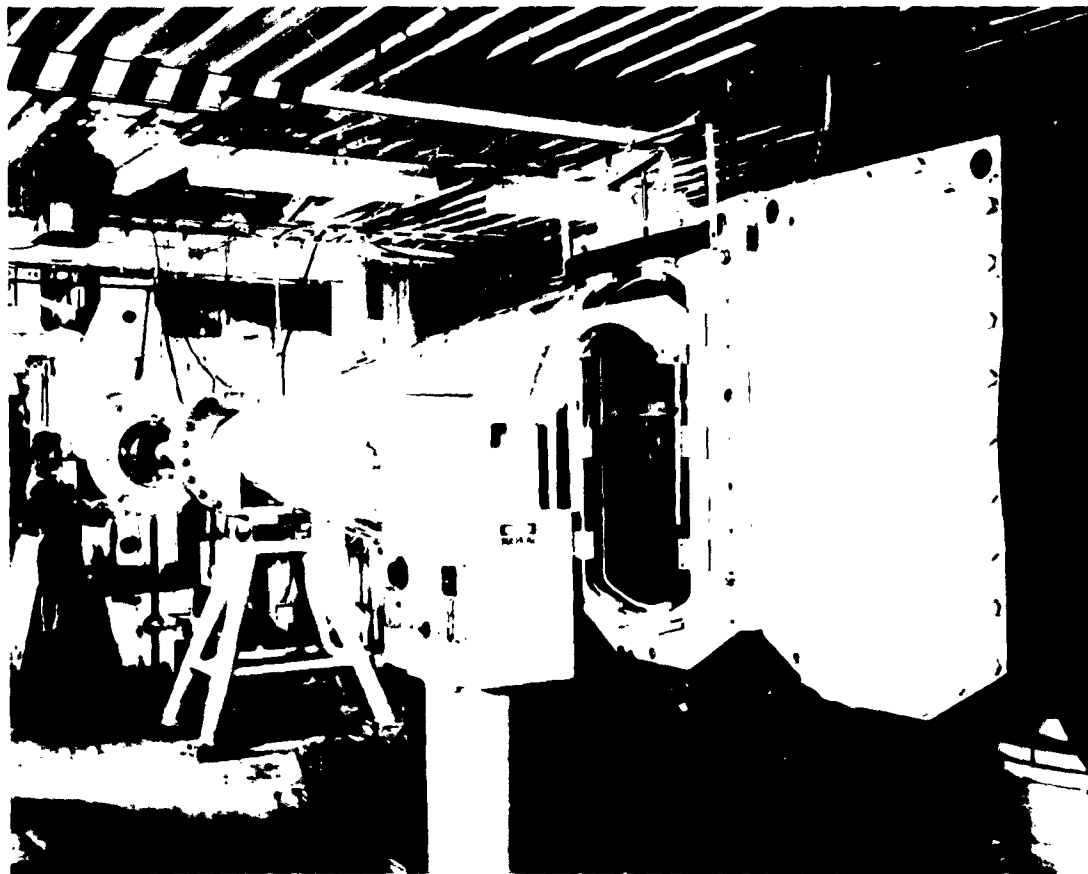


Arc Chamber, Nozzle, and Test Section

Fig. 1 Tunnel Hotshot 1, a 16-in.-diam Hypervelocity Wind Tunnel



Assembly



Arc Chamber, Nozzle, and Test Section

Fig. 1 The 50-Inch Hypervelocity Wind Tunnel, Tunnel Hotshot 2

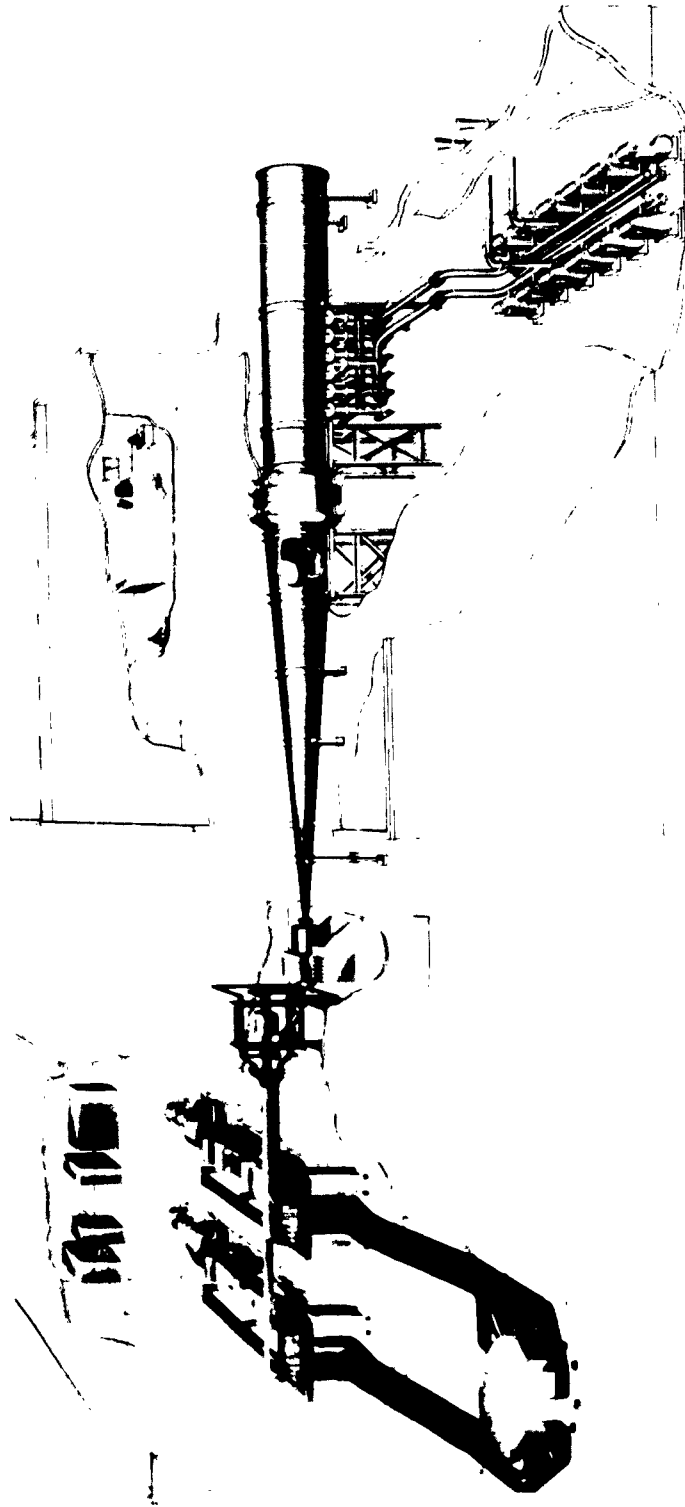


Fig. 3 The 100-Inch Hypervelocity Wind Tunnel (Tunnel F)

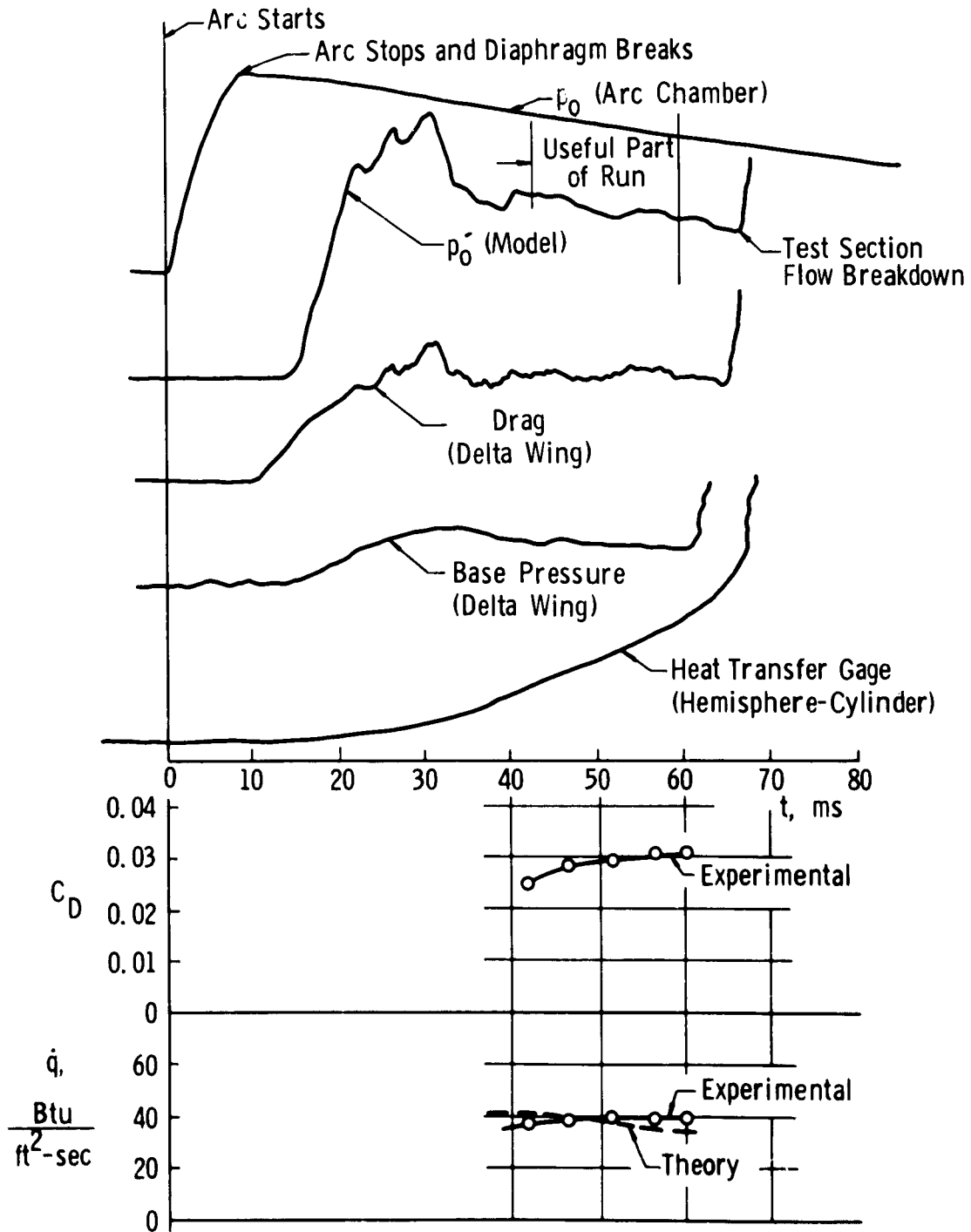
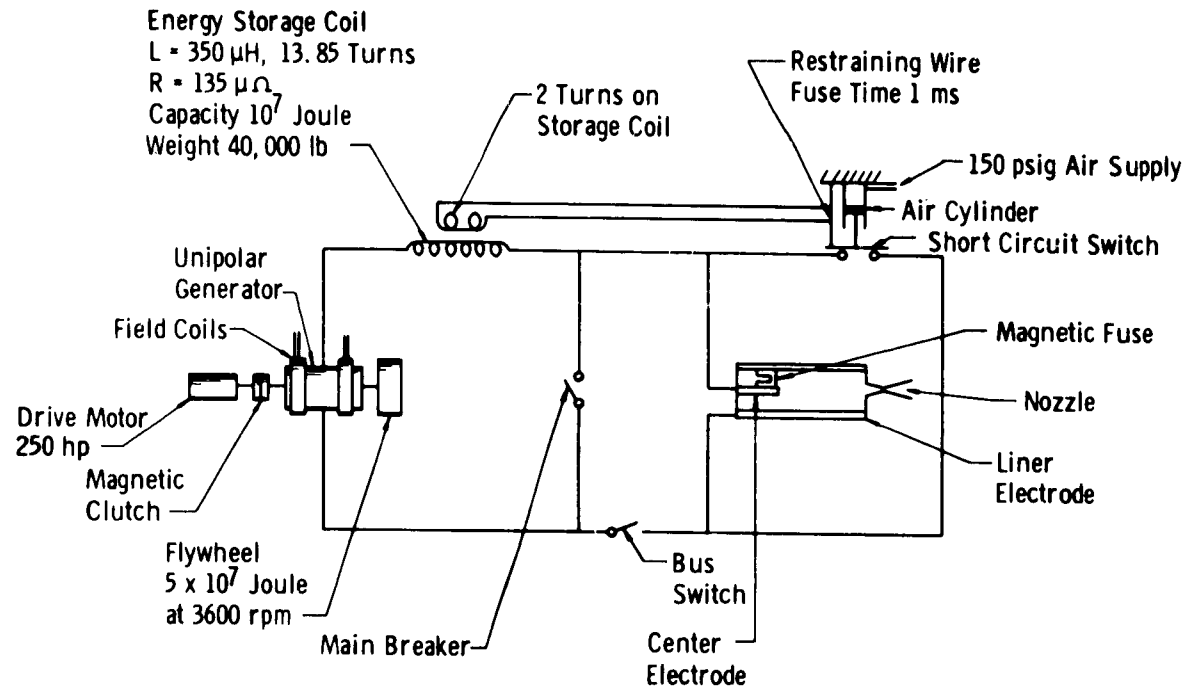
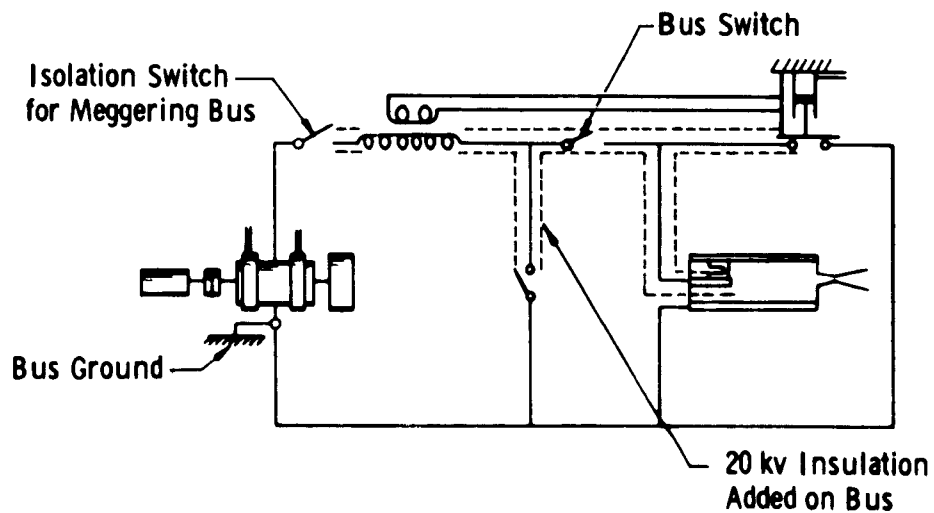


Fig. 4 Typical Oscillograph Traces and Timewise Variation of C_D and q in the 50-Inch Hypervelocity Tunnel (Hotshot 2)



a. Before Grounding



b. After Grounding

Fig. 5 Schematic of Inductance Energy Storage System of the 50-Inch Hypervelocity Tunnel (Hotshot 2)

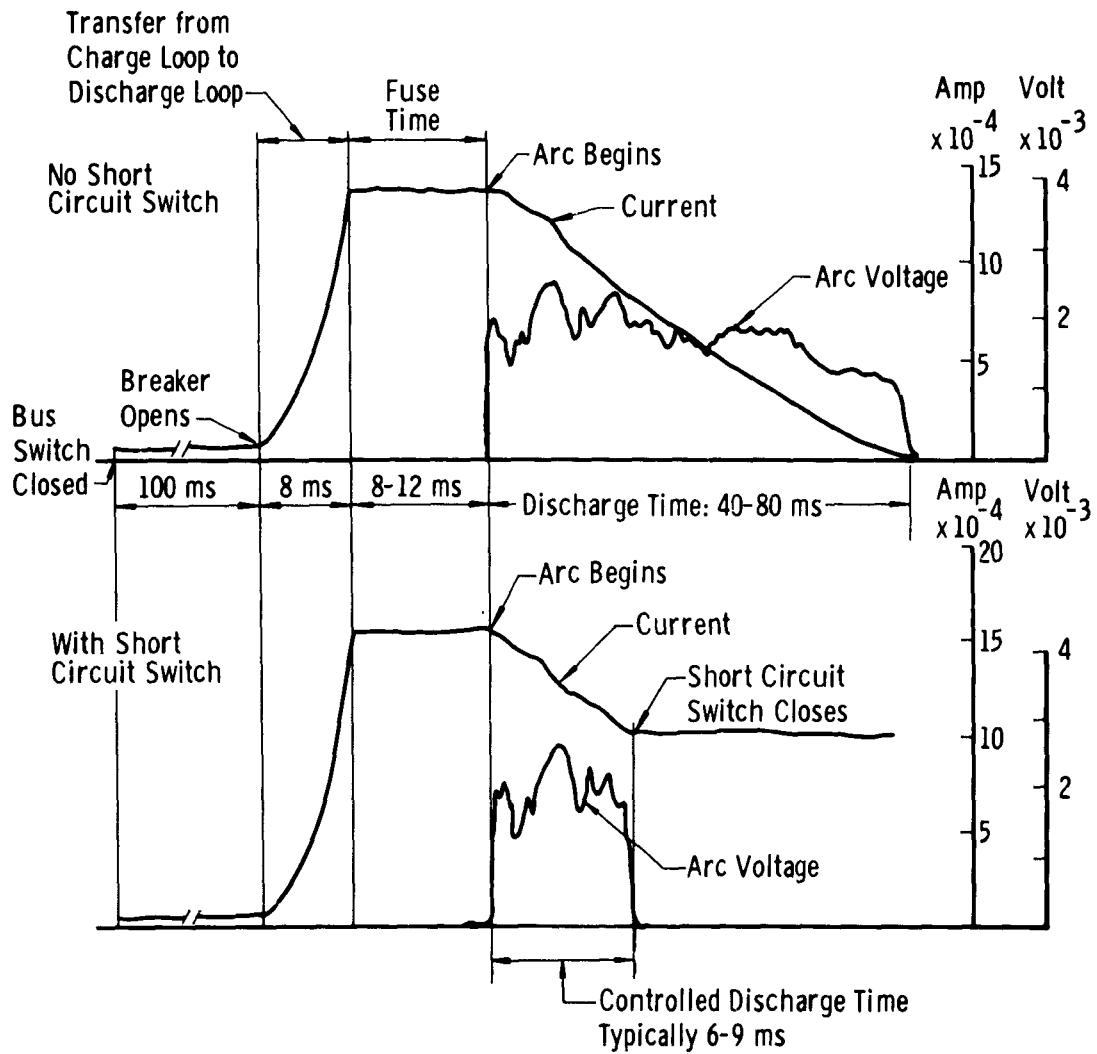
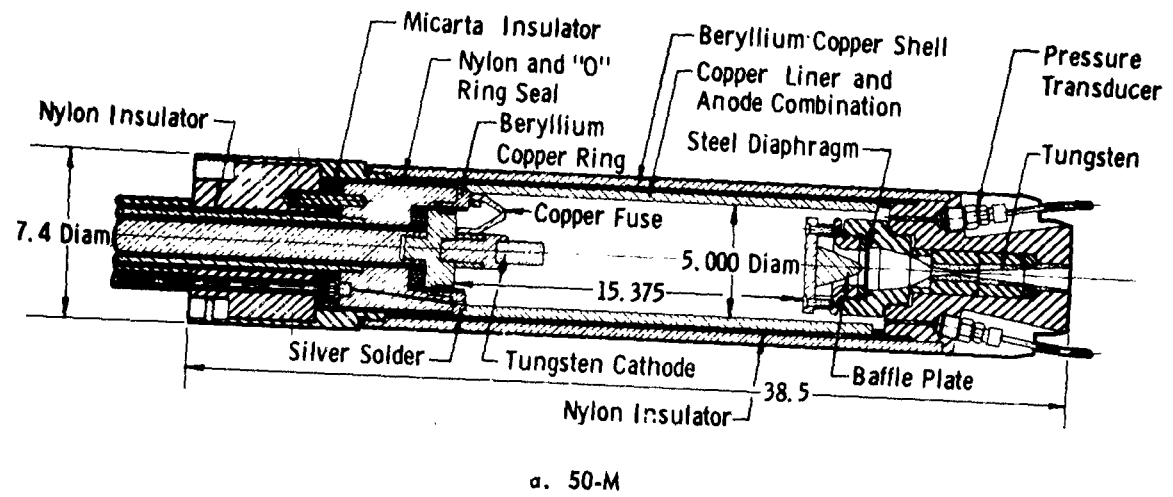


Fig. 6 Typical Current and Voltage Traces without and with Short Circuit Switch (Hotshot 2)



All Dimensions in Inches.

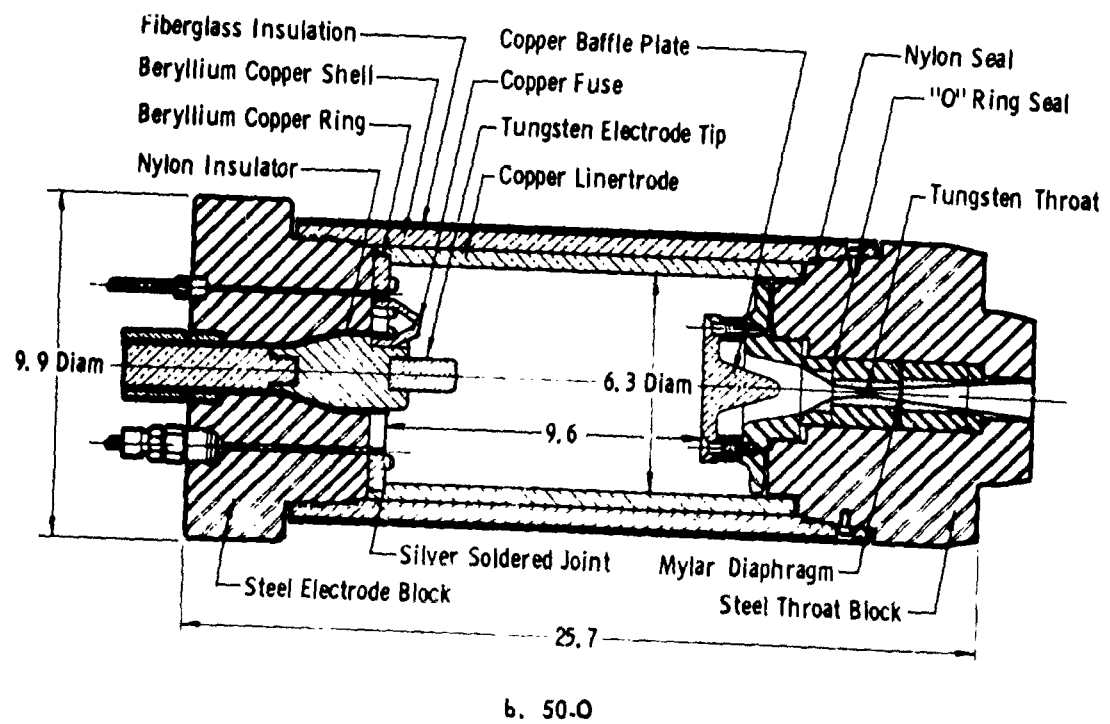


Fig. 7 Coaxial Arc Chambers of the 50-Inch Hypervelocity Tunnel (Hotshot 2)

Nitrogen: $(\rho_0)_i = 80-100$ Amagat
 $(T_0)_{max} = 3000-4000^{\circ}K$

$M_{\infty} = 18-22$
 $d^* = 0.188-0.281$ in.

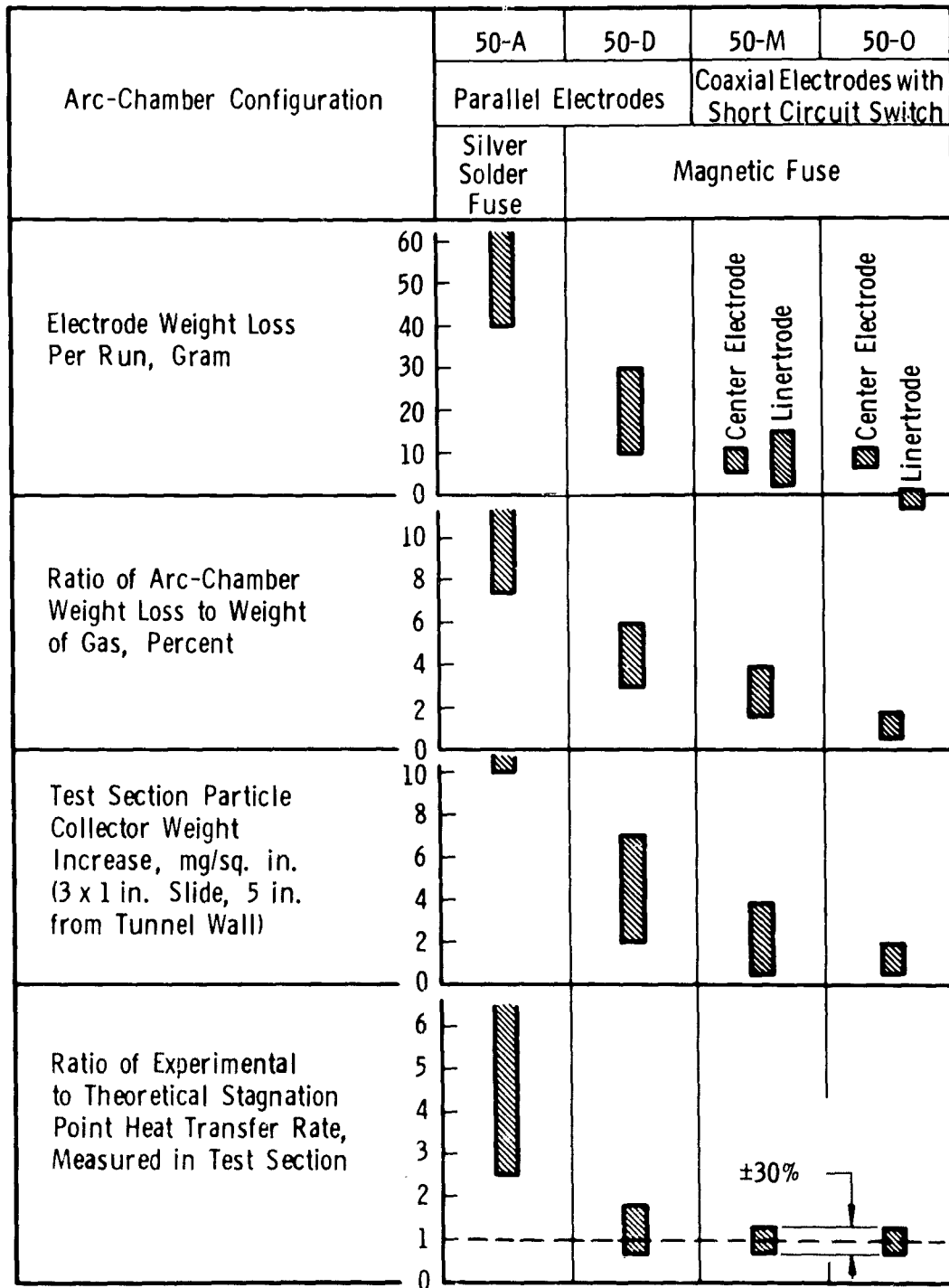


Fig. 8 Summary of Test Results Obtained with Various Arc Chambers in the 50-Inch Hypervelocity Tunnel (Hotshot 2)

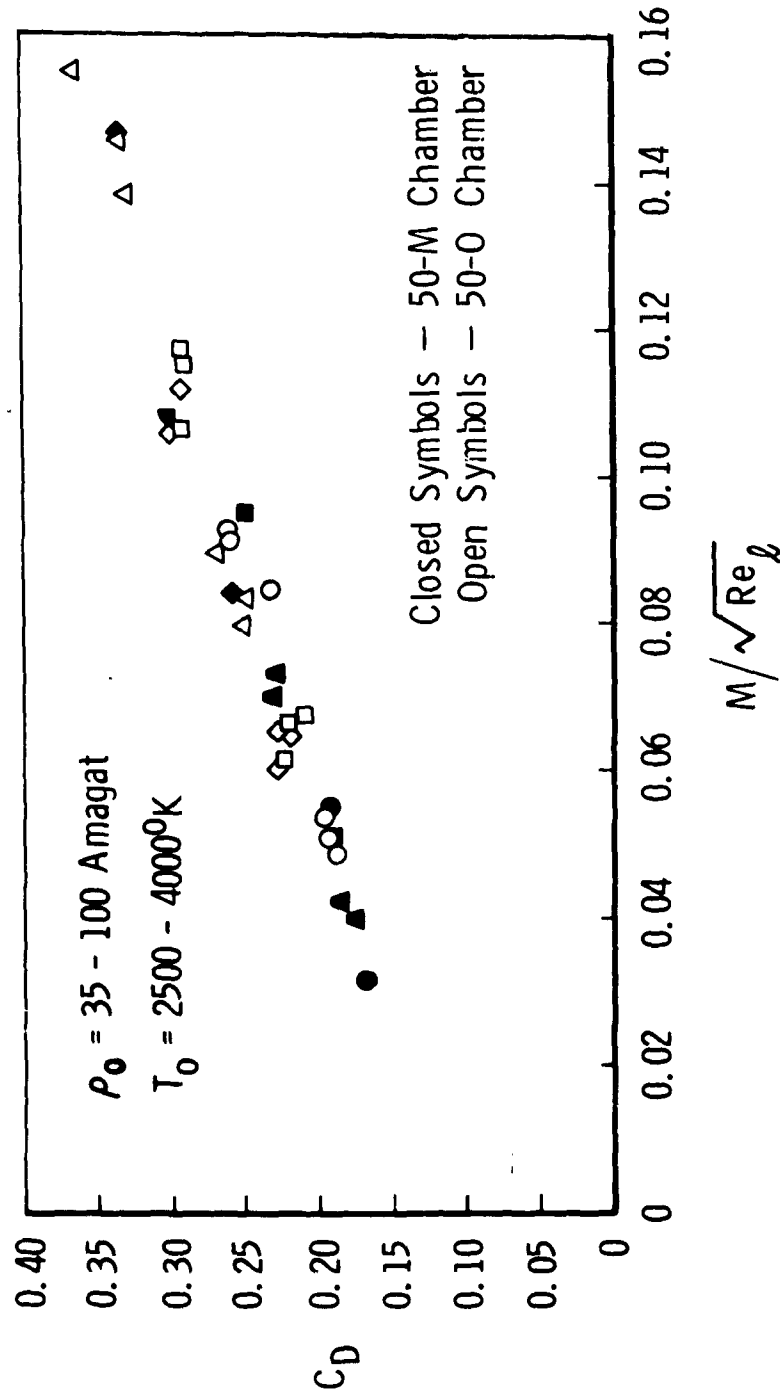


Fig. 9 Drag Coefficients from Two Blunt 9-deg Cones, Nose to Base Radius Ratio of 0.3, Base Radii of 1-in. and 3-in. (Hotshot 2)

Nominal Arc Chamber Dimensions
 Internal Diameter, 2.5 in.
 Length, 6.5 in.³
 Volume, 30 in.³
 Internal Surface Area, 60 in.²
 Pressure Rating, 30,000 psi

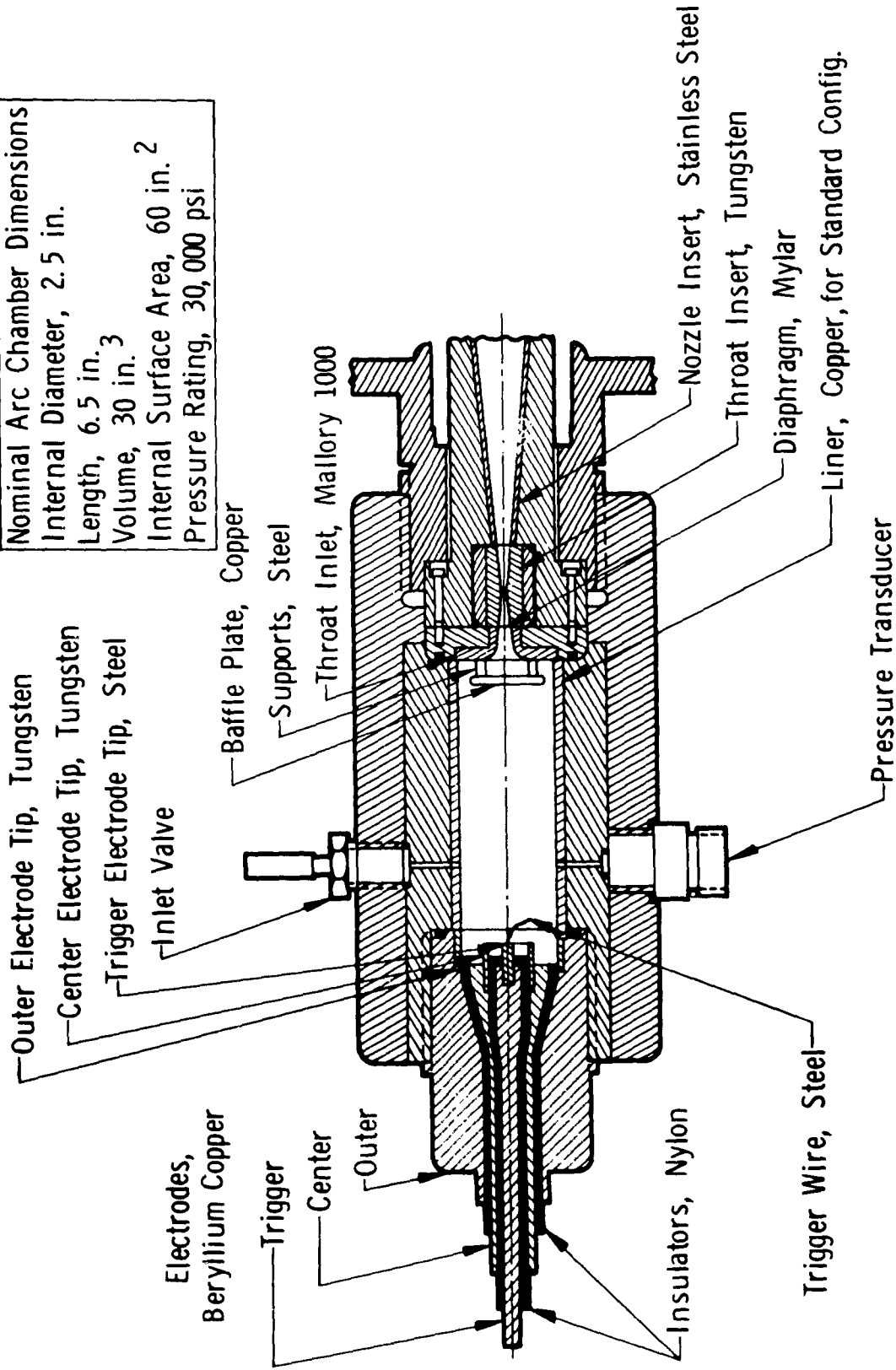


Fig. 10 Arc Chamber 16-C of the 16-in.-diam Hypervelocity Tunnel, Hotshot 1

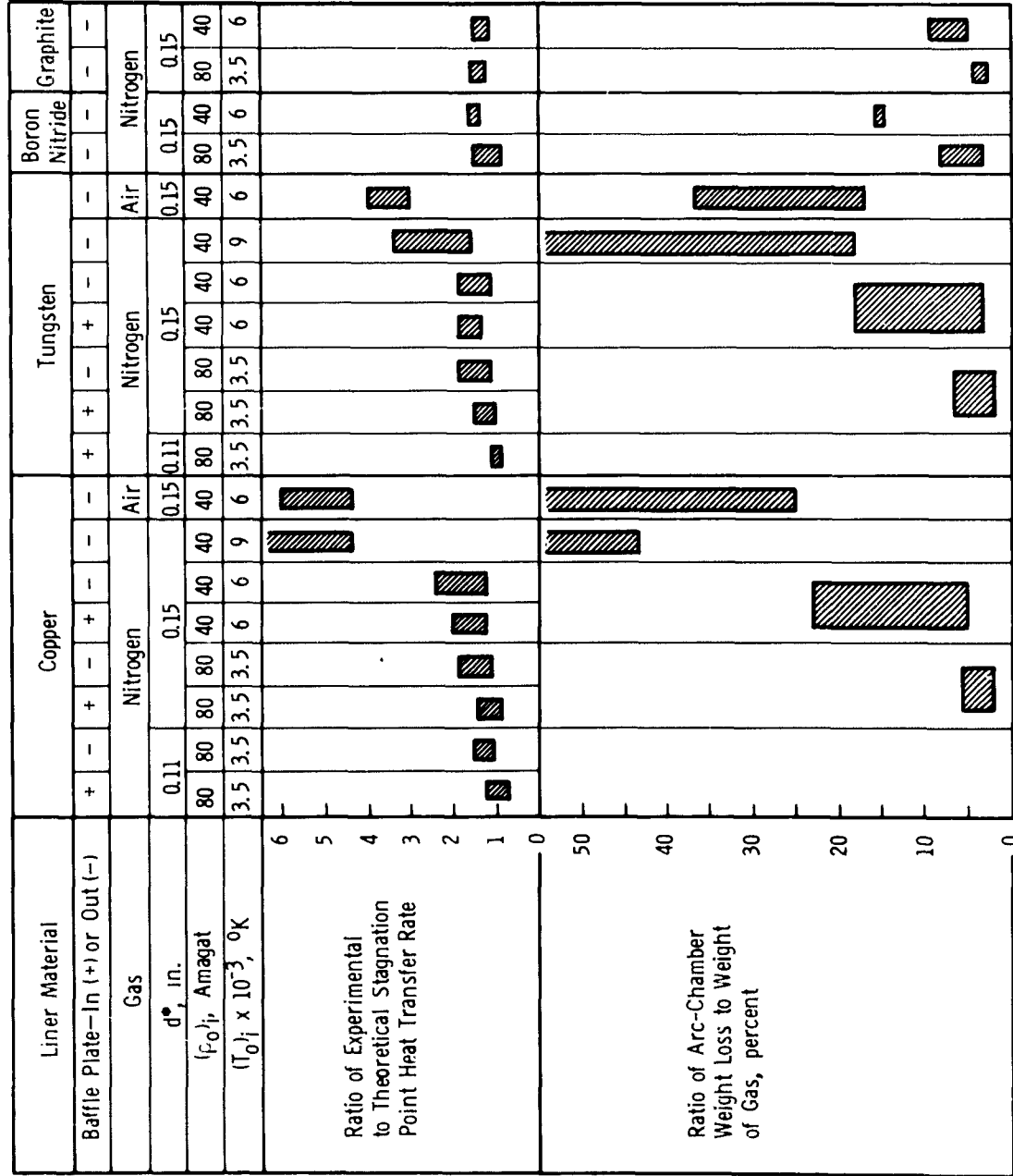


Fig. 11 Summary of Test Results with Various Arc-Chamber Liner Materials in Tunnel Hotshot 1

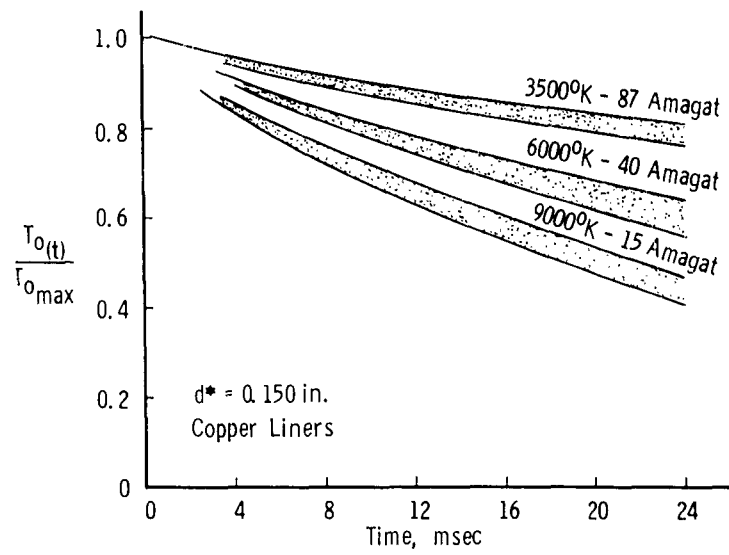


Fig. 12 Temperature Decay in the 16-C Chamber (Hotshot 1)

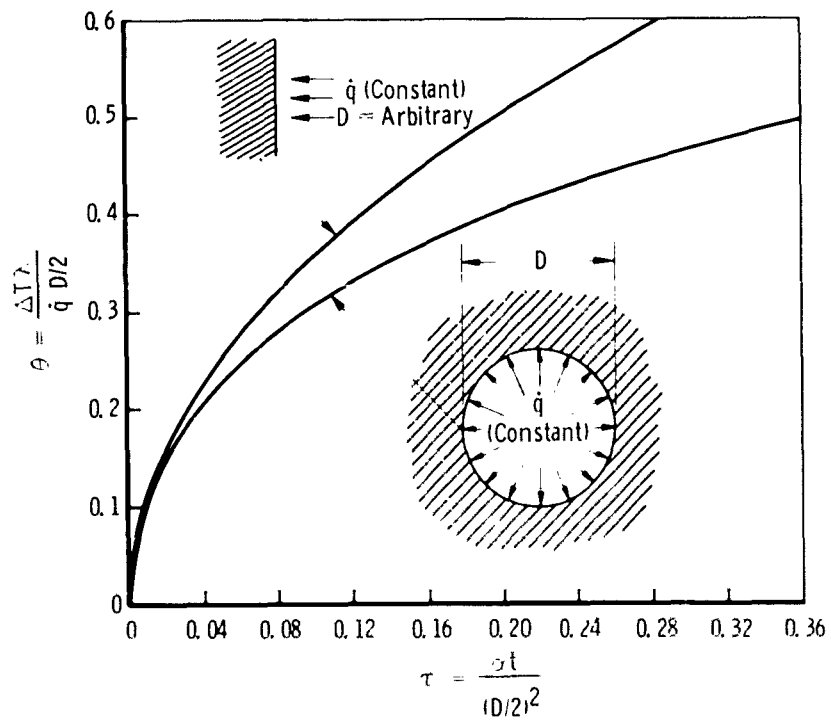


Fig. 13 Temperature Rise in Semi-Infinite Solid and Infinite Hollow Cylinder

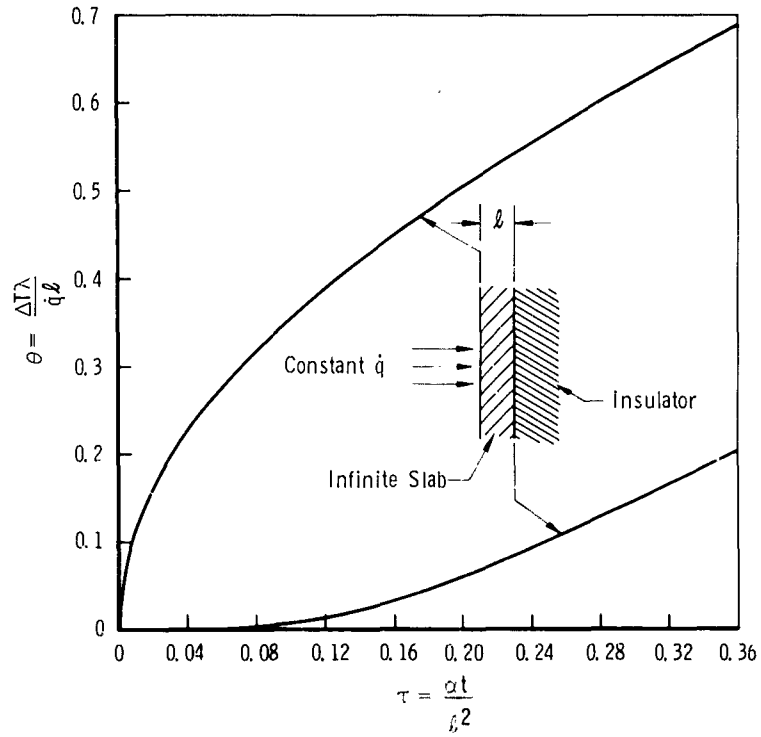


Fig. 14 Temperature Rise in Infinite Slab on Insulator

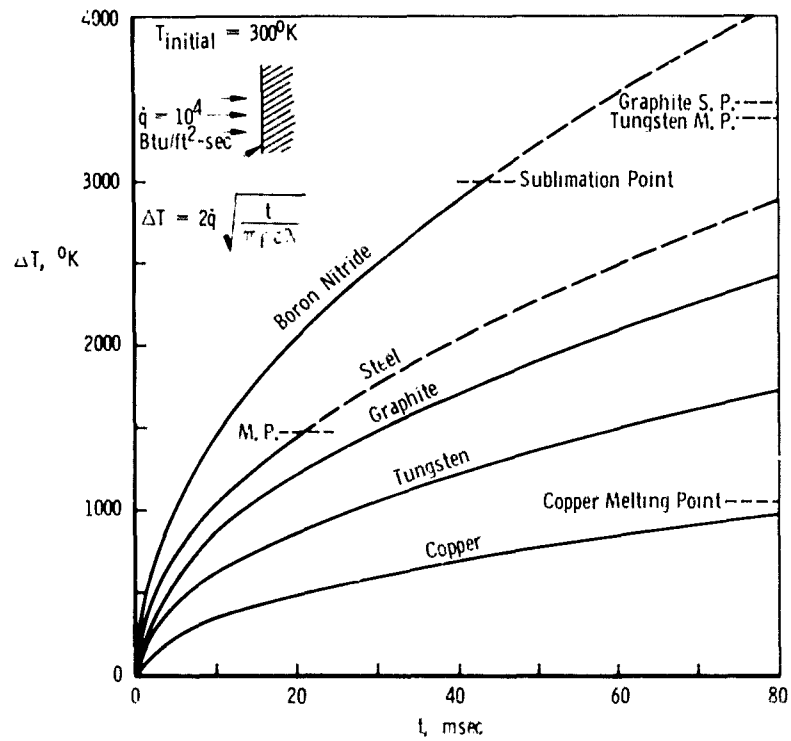


Fig. 15 Temperature Rise in Semi-Infinite Wall for Different Materials

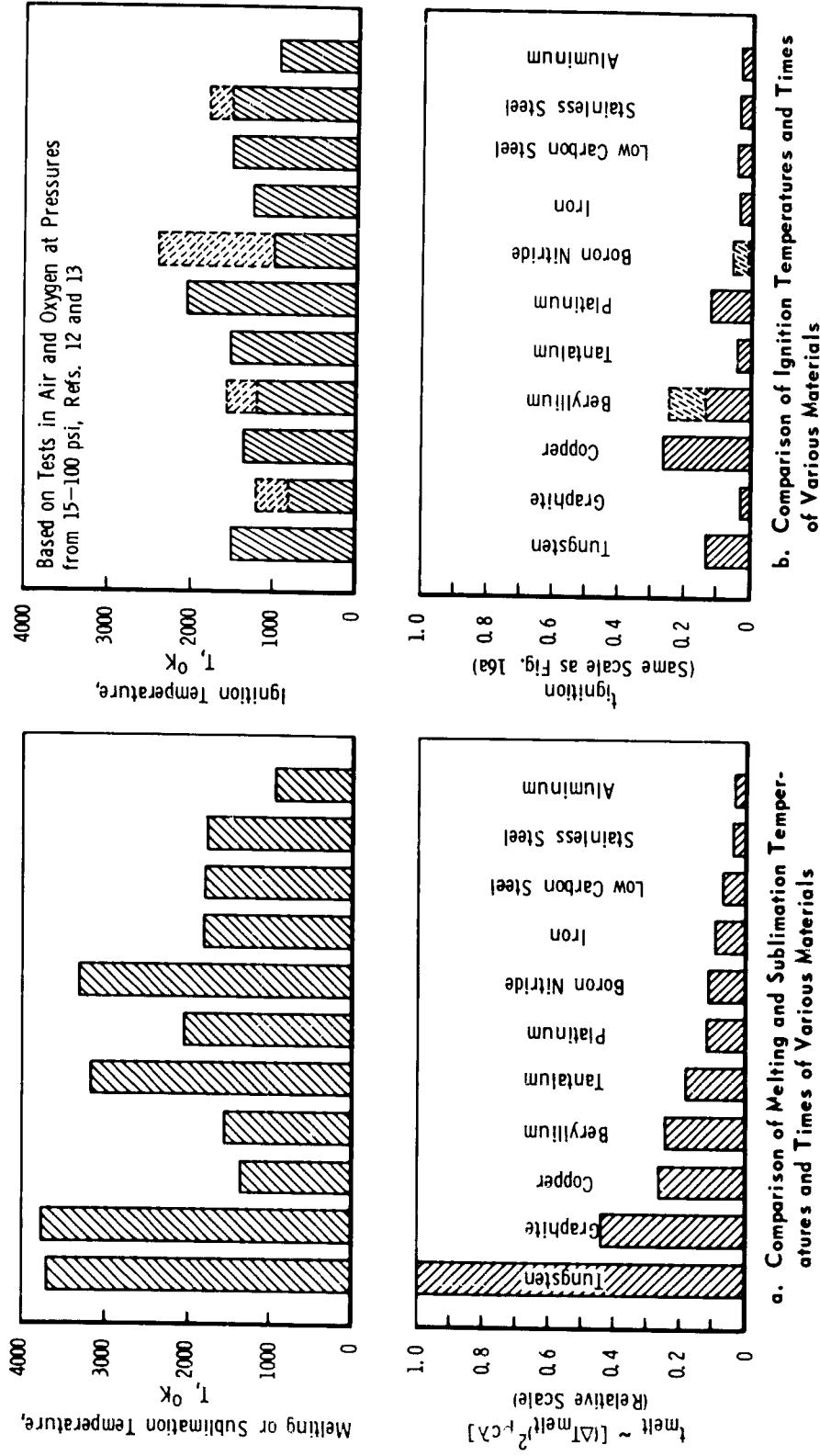


Fig. 16 Comparison of Liner Materials

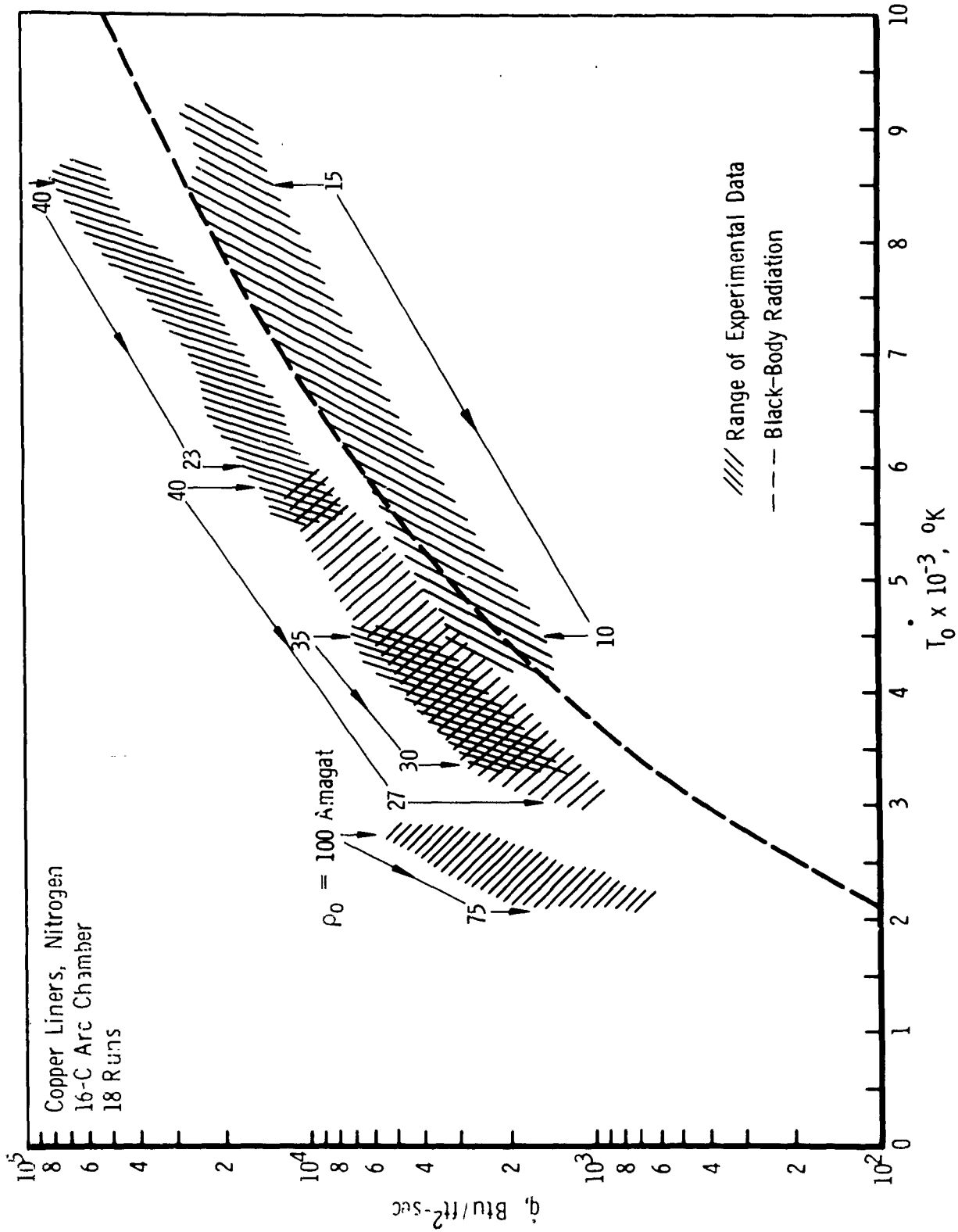


Fig. 17 Experimental Arc-Chamber Heat Loss in Tunnel Hotshot 1

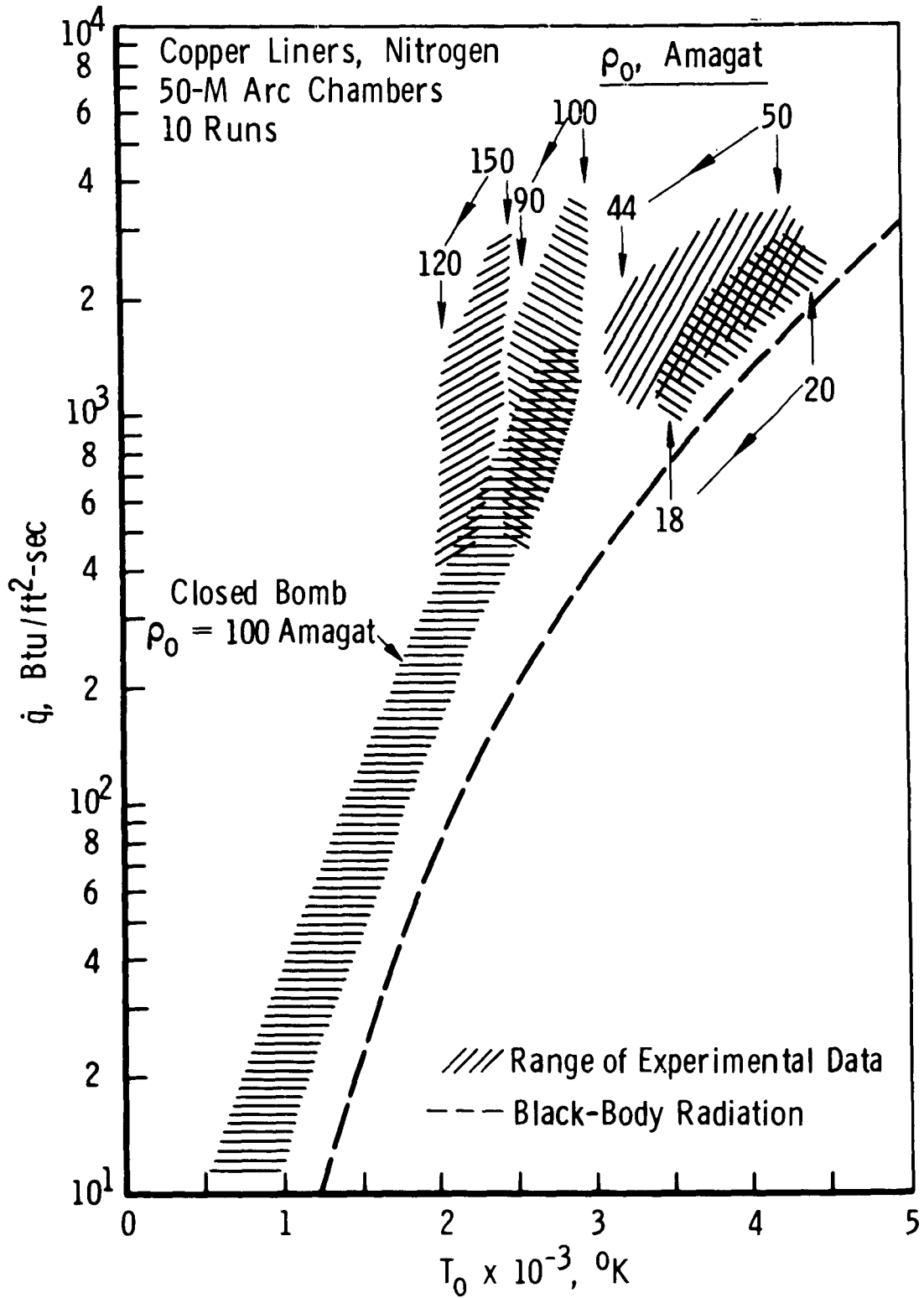


Fig. 18 Experimental Arc-Chamber Heat Loss in the 50-Inch Hypervelocity Tunnel (Hotshot 2)

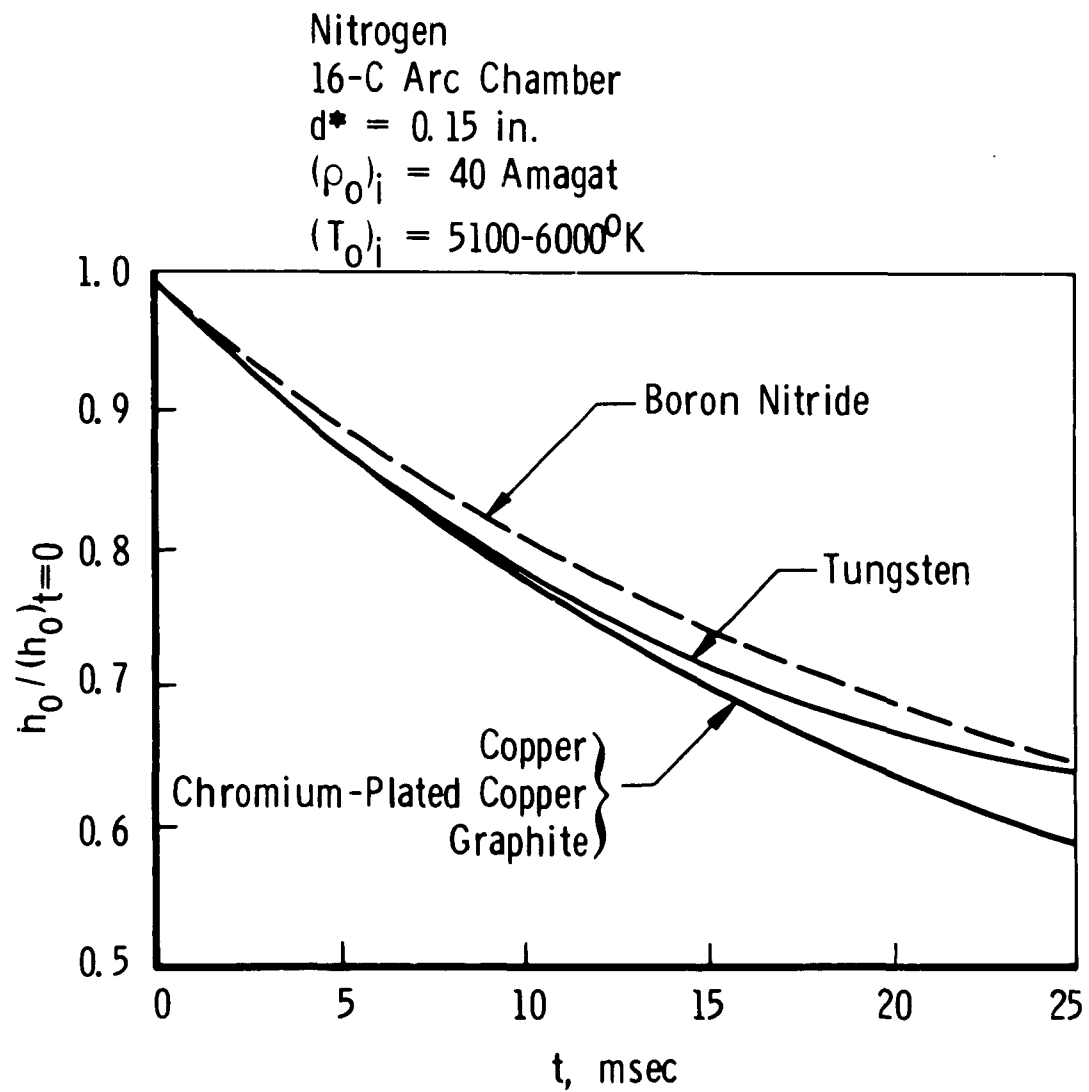


Fig. 19 Experimental Enthalpy Decay with Various Liner Materials (Hotshot 1)

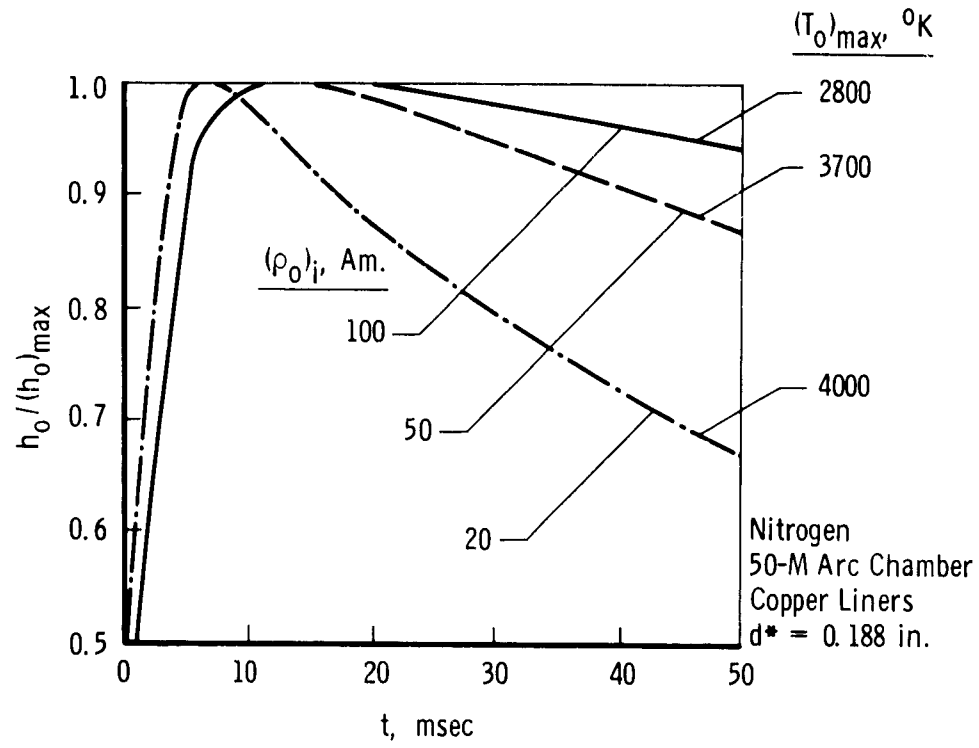


Fig. 20 Experimental Enthalpy Decay for Three Different Densities (Hotshot 2)

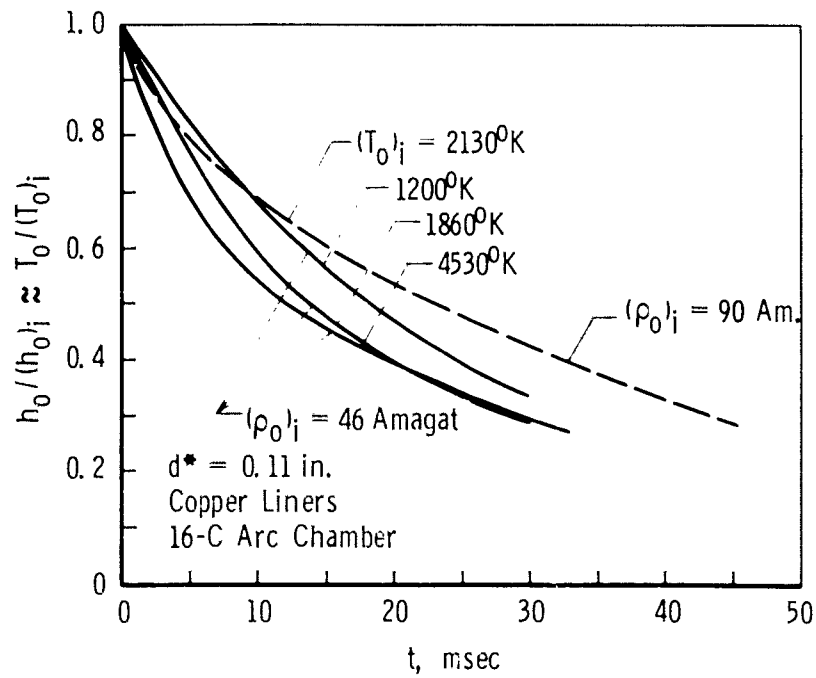


Fig. 21 Experimental Enthalpy Decay with Helium (Hotshot 1)

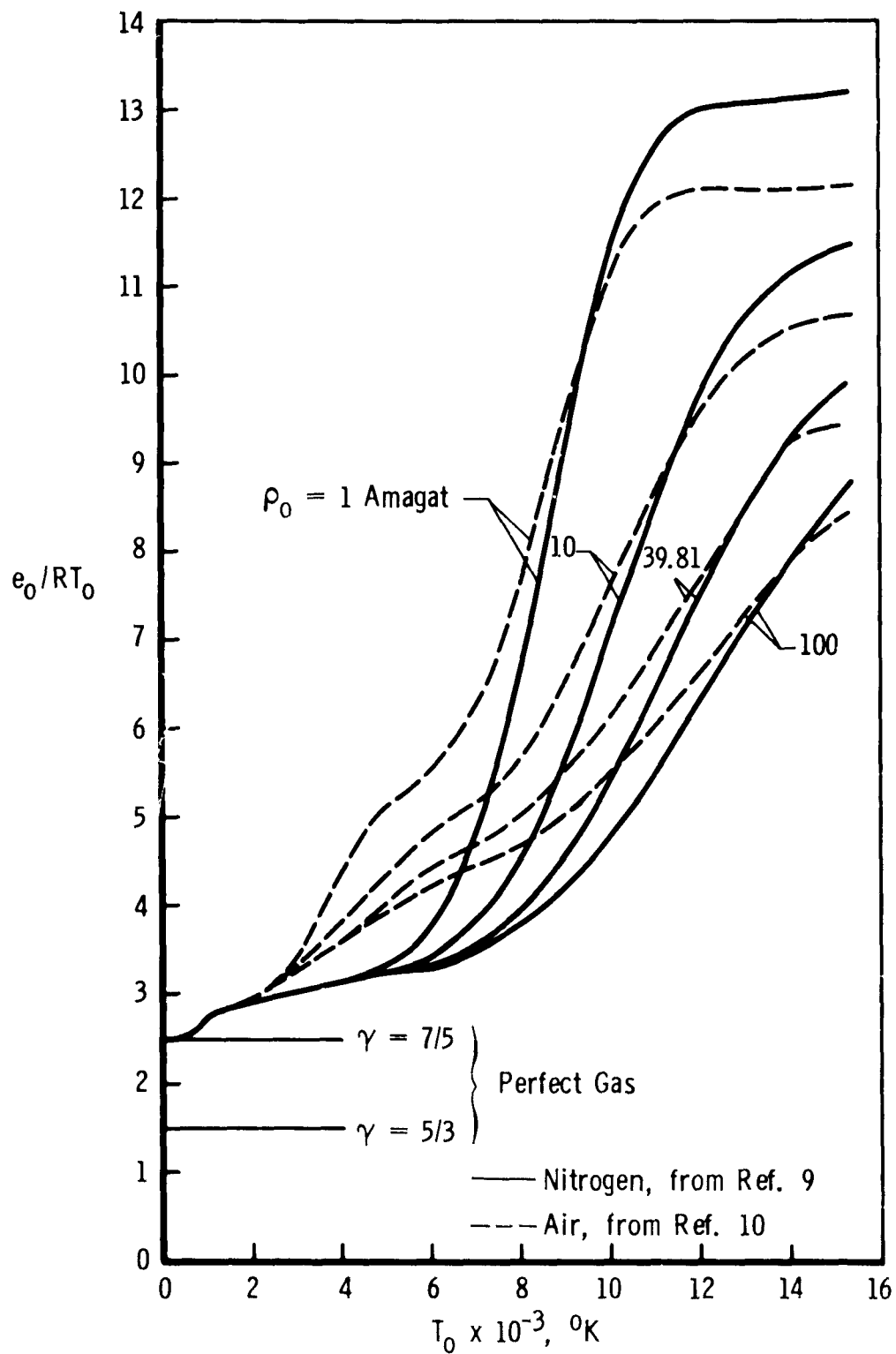


Fig. 22 Internal Energy for Air and Nitrogen

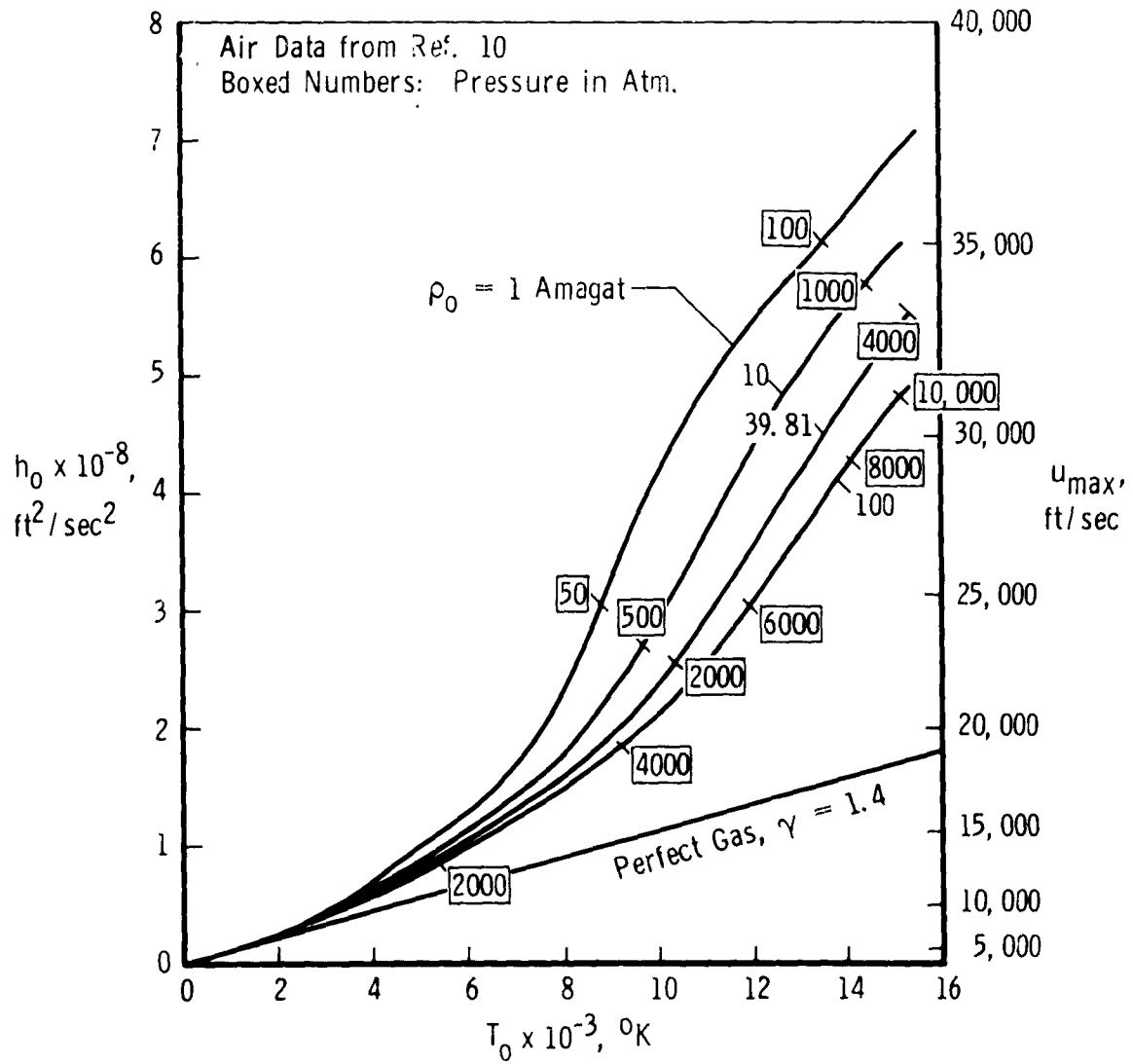


Fig. 23 Enthalpy and Maximum Velocity for Air

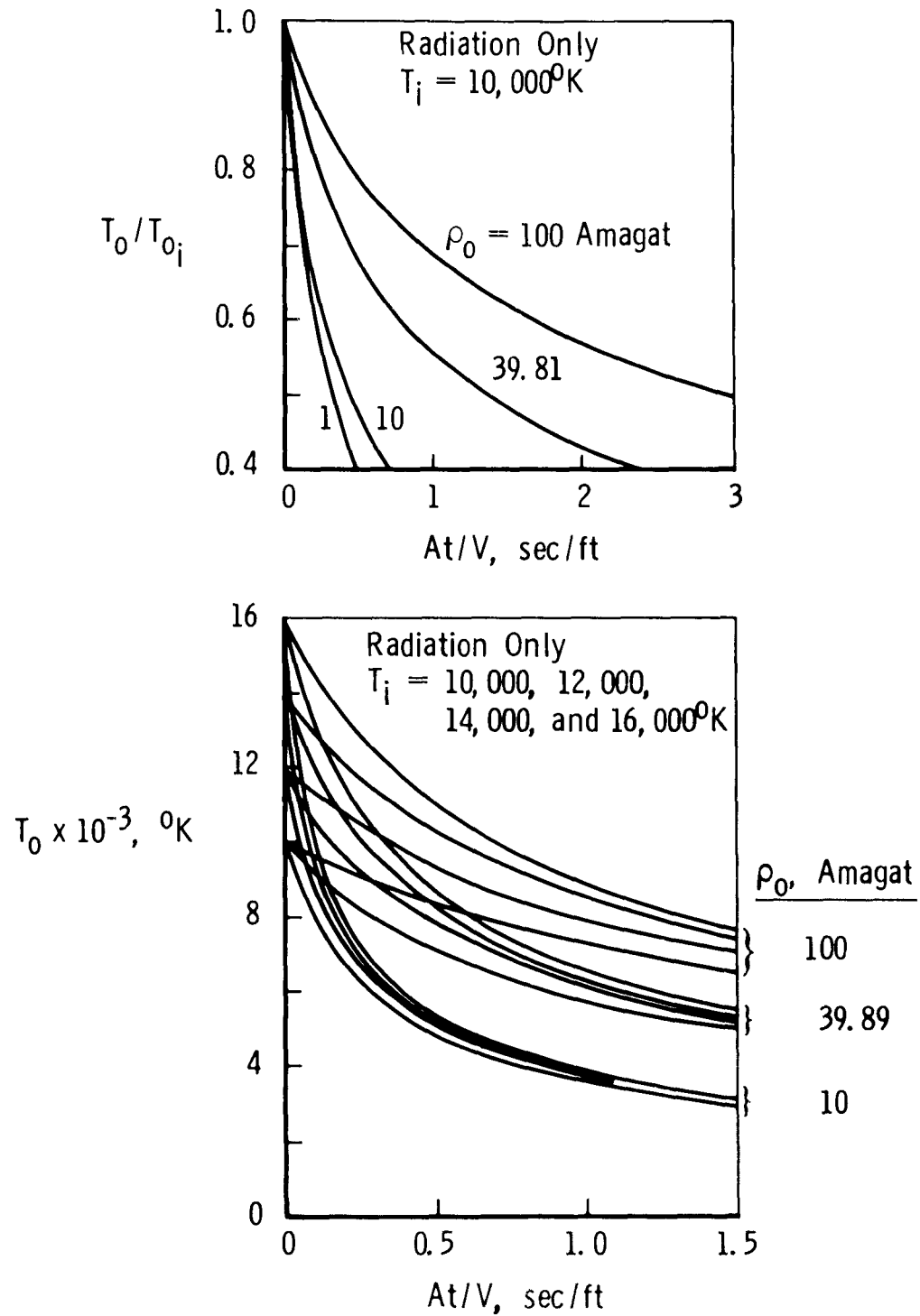


Fig. 24 Temperature Decay Caused by Radiation for Air in Closed Reservoir

Test Section	E_{stored}	V	Est. / V
Hotshot 1 16-in. diam	10^6 Joule	0.018 ft ³	57.5×10^6 Joule/ft ³
Hotshot 2 50-in. diam	10×10^6 Joule	0.21 ft ³	48×10^6 Joule/ft ³
Tunnel F 100-in. diam	100×10^6 Joule	1.08 ft ³	93×10^6 Joule/ft ³

Air, Radiation Heat Losses Only

At/V, sec/ft

E, Effective Energy in Air, Joule

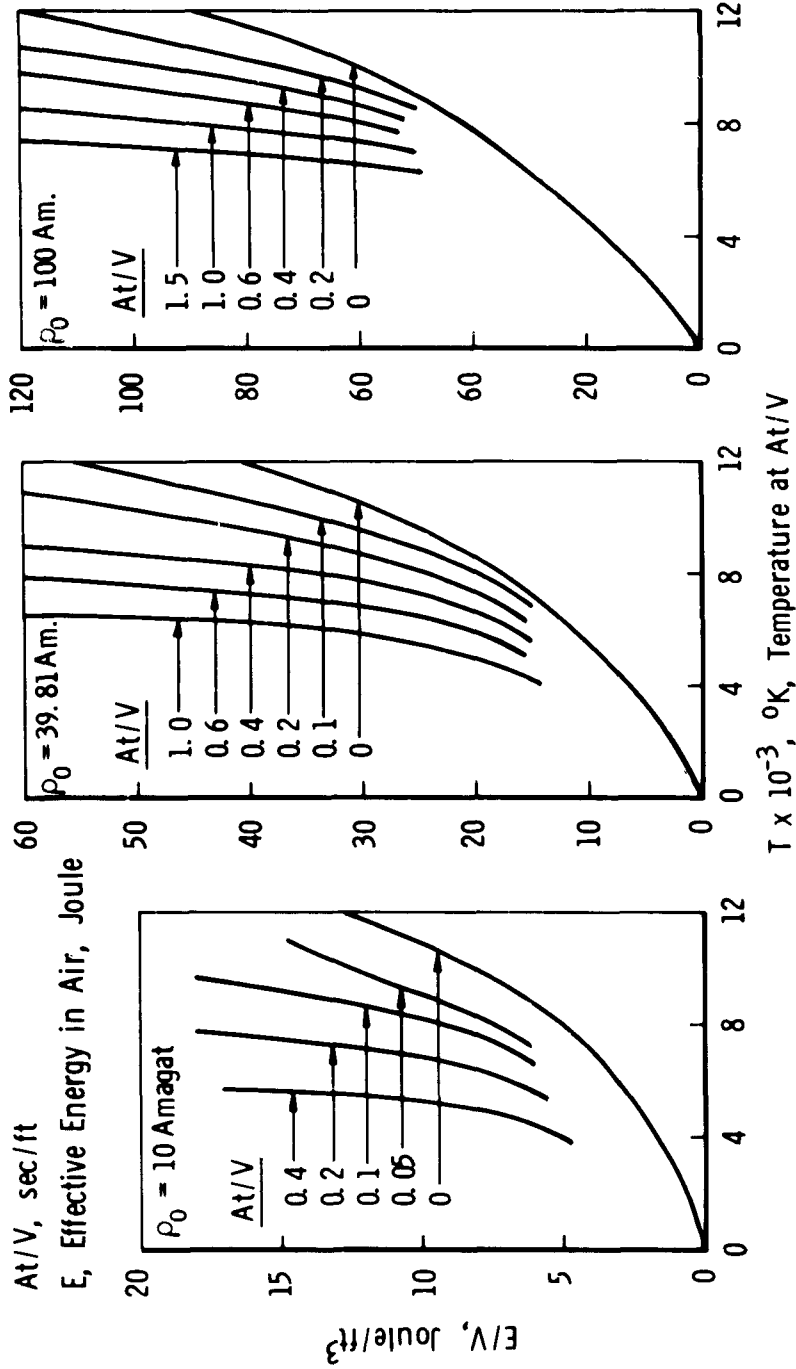


Fig. 25 Required Energy for Desired Air Temperature at Time of Test

<p>Arnold Engineering Development Center Arnold Air Force Station, Tennessee Rpt. No. AFDC-TDR-62-50 FURTHER DEVELOPMENT OF CAPACITANCE- AND INDUCTANCE-DRIVEN HOT- SHOT TUNNELS. March 1962, 36 p. incl 15 refs., illus., tables.</p> <p>Unclassified Report</p> <p>Significant developments of the hotshot tunnels in the von Kármán Gas Dynamics Facility, Arnold Engineering Devel- opment Center, Arnold Air Force Station, Tennessee, since the First National Symposium on Hypervelocity Techniques are described. An arc chamber with coaxial electrodes was developed for the inductance-driven 50-inch Hyper- velocity Tunnel (Hotshot 2). Combined with a short-circuit switch, to reduce the discharge time, this configuration re- sulted in a significant decrease in flow contamination. Force tests in the Mach number range from 16-22 at stagnation temperatures from 3000-4000°K and stagnation pressures</p>	<p>1 Wind tunnels 2 Design 3 Growth 4 Hypervelocity I AFSC Program Area 750A, Project 8952, Task 89512 II Contract AF 40(600)-300 S/A 24(61-73) Tenn. III. ARO, Inc., Arnold AF Sta. IV. J. A. van der Bliek V. Available from OTS VI In ASTIA collection</p>	<p>Arnold Engineering Development Center Arnold Air Force Station, Tennessee Rpt. No. AFDC-TDR-62-50 FURTHER DEVELOPMENT OF CAPACITANCE- AND INDUCTANCE-DRIVEN HOT- SHOT TUNNELS. March 1962, 36 p. incl 15 refs., illus., tables.</p> <p>Unclassified Report</p> <p>Significant developments of the hotshot tunnels in the von Kármán Gas Dynamics Facility, Arnold Engineering Devel- opment Center, Arnold Air Force Station, Tennessee, since the First National Symposium on Hypervelocity Techniques are described. An arc chamber with coaxial electrodes was developed for the inductance-driven 50-inch Hyper- velocity Tunnel (Hotshot 2). Combined with a short-circuit switch, to reduce the discharge time, this configuration re- sulted in a significant decrease in flow contamination. Force tests in the Mach number range from 16-22 at stagnation temperatures from 3000-4000°K and stagnation pressures</p>	<p>1. Wind tunnels 2. Design 3. Growth 4. Hypervelocity I. AFSC Program Area 750A, Project 8952, Task 89512 II. Contract AF 40(600)-300 S/A 24(61-73) III. ARO, Inc., Arnold AF Sta, Tenn. IV. J. A. van der Bliek V. Available from OTS VI. In ASTIA collection</p>
<p>from 10,000-20,000 psi were in good agreement with re- sults from other tunnels. An arc-chamber liner material study was carried out in the capacitance-driven Tunnel Hotshot 1. The materials tested included copper, boron nitride, graphite, tungsten, and chrome-plated copper. The heat losses through the arc-chamber walls of Hotshot 1, determined from runs at stagnation temperatures from 3000-9000°K, are presented, and their implications on hot- shot tunnel operation are discussed.</p>		<p>from 10,000-20,000 psi were in good agreement with re- sults from other tunnels. An arc-chamber liner material study was carried out in the capacitance-driven Tunnel Hotshot 1. The materials tested included copper, boron nitride, graphite, tungsten, and chrome-plated copper. The heat losses through the arc-chamber walls of Hotshot 1, determined from runs at stagnation temperatures from 3000-9000°K, are presented, and their implications on hot- shot tunnel operation are discussed.</p>	

<p>Arnold Engineering Development Center Arnold Air Force Station, Tennessee Rpt. No. AEDC-TDR-62-50. FURTHER DEVELOPMENT OF CAPACITANCE- AND INDUCTANCE-DRIVEN HOT- SHOT TUNNELS. March 1962, 36 p. incl 15 refs., illus., tables.</p> <p>Unclassified Report</p> <p>Significant developments of the hotshot tunnels in the von Kármán Gas Dynamics Facility, Arnold Engineering Development Center, Arnold Air Force Station, Tennessee, since the First National Symposium on Hypervelocity Techniques are described. An arc chamber with coaxial electrodes was developed for the inductance-driven 50-inch Hypervelocity Tunnel (Hotshot 2). Combined with a short-circuit switch, to reduce the discharge time, this configuration resulted in a significant decrease in flow contamination. Force tests in the Mach number range from 16-22 at stagnation temperatures from 3000-4000°K and stagnation pressures</p>	<p>1 Wind tunnels 2 Design 3 Growth 4 Hypervelocity</p> <p>I AFSC Program Area 750A, Project 8852, Task 89512 II Contract AF 40(600)-800 S/A 24(61-73) III ARO, Inc., Arnold AF Sta, Tenn. IV J. A. van der Bliek V. Available from OTS VI ASTIA collection</p>	<p>Arnold Engineering Development Center Arnold Air Force Station, Tennessee Rpt. No. AEDC-TDR-62-50. FURTHER DEVELOPMENT OF CAPACITANCE- AND INDUCTANCE-DRIVEN HOT- SHOT TUNNELS. March 1962, 36 p. incl 15 refs., illus., tables.</p> <p>Unclassified Report</p> <p>Significant developments of the hotshot tunnels in the von Kármán Gas Dynamics Facility, Arnold Engineering Development Center, Arnold Air Force Station, Tennessee, since the First National Symposium on Hypervelocity Techniques are described. An arc chamber with coaxial electrodes was developed for the inductance-driven 50-inch Hypervelocity Tunnel (Hotshot 2). Combined with a short-circuit switch, to reduce the discharge time, this configuration resulted in a significant decrease in flow contamination. Force tests in the Mach number range from 16-22 at stagnation temperatures from 3000-4000°K and stagnation pressures</p>	<p>1. Wind tunnels 2. Design 3. Growth 4. Hypervelocity</p> <p>I. AFSC Program Area 750A, Project 8852, Task 89512 II. Contract AF 40(600)-800 S/A 24(61-73) III. ARO, Inc., Arnold AF Sta, Tenn. IV. J. A. van der Bliek V. Available from OTS VI. In ASTIA collection</p>
<p>from 10,000-20,000 psi were in good agreement with results from other tunnels. An arc-chamber liner material study was carried out in the capacitance-driven Tunnel Hotshot 1. The materials tested included copper, boron nitride, graphite, tungsten, and chrome-plated copper. The heat losses through the arc-chamber walls of Hotshot 1, determined from runs at stagnation temperatures from 3000-9000°K, are presented, and their implications on hot-shot tunnel operation are discussed.</p>	<p>from 10,000-20,000 psi were in good agreement with results from other tunnels. An arc-chamber liner material study was carried out in the capacitance-driven Tunnel Hotshot 1. The materials tested included copper, boron nitride, graphite, tungsten, and chrome-plated copper. The heat losses through the arc-chamber walls of Hotshot 1, determined from runs at stagnation temperatures from 3000-9000°K, are presented, and their implications on hot-shot tunnel operation are discussed.</p>	<p>from 10,000-20,000 psi were in good agreement with results from other tunnels. An arc-chamber liner material study was carried out in the capacitance-driven Tunnel Hotshot 1. The materials tested included copper, boron nitride, graphite, tungsten, and chrome-plated copper. The heat losses through the arc-chamber walls of Hotshot 1, determined from runs at stagnation temperatures from 3000-9000°K, are presented, and their implications on hot-shot tunnel operation are discussed.</p>	<p>from 10,000-20,000 psi were in good agreement with results from other tunnels. An arc-chamber liner material study was carried out in the capacitance-driven Tunnel Hotshot 1. The materials tested included copper, boron nitride, graphite, tungsten, and chrome-plated copper. The heat losses through the arc-chamber walls of Hotshot 1, determined from runs at stagnation temperatures from 3000-9000°K, are presented, and their implications on hot-shot tunnel operation are discussed.</p>

<p>Arnold Engineering Development Center Arnold Air Force Station, Tennessee Rpt No. AEDC-TDR-62-50 FURTHER DEVELOPMENT OF CAPACITANCE- AND INDUCTANCE-DRIVEN HOT- SHOT TUNNELS March 1962, 36 p. incl 15 refs., illus., tables</p> <p>Unclassified Report</p> <p>Significant developments of the hotshot tunnels in the von Kármán Gas Dynamics Facility, Arnold Engineering Devel- opment Center, Arnold Air Force Station, Tennessee, since the First National Symposium on Hypervelocity Techniques are described. An arc chamber with coaxial electrodes was developed for the inductance-driven 50-Inch Hyper- velocity Tunnel (Hotshot 2). Combined with a short-circuit switch, to reduce the discharge time, this configuration re- sulted in a significant decrease in flow contamination. For- tests in the Mach number range from 16-22 at stagnation temperatures from 3000-4000°K and stagnation pressures</p>	<p>1 Wind tunnels 2 Design 3 Growth 4 Hypervelocity I AFSC Program Area 750A, Project 8852, Task 88512 Contract AF 40(600)-800 S/A 24(61-73) III ARO, Inc., Arnold AF Sta, Tenn. IV J. A. van der Bliek V Available from OTS VI In ASTIA collection</p>	<p>Arnold Engineering Development Center Arnold Air Force Station, Tennessee Rpt No. AEDC-TDR-62-50 FURTHER DEVELOPMENT OF CAPACITANCE- AND INDUCTANCE-DRIVEN HOT- SHOT TUNNELS March 1962, 36 p. incl 15 refs., illus., tables</p> <p>Unclassified Report</p> <p>Significant developments of the hotshot tunnels in the von Kármán Gas Dynamics Facility, Arnold Engineering Devel- opment Center, Arnold Air Force Station, Tennessee, since the First National Symposium on Hypervelocity Techniques are described. An arc chamber with coaxial electrodes was developed for the inductance-driven 50-Inch Hyper- velocity Tunnel (Hotshot 2). Combined with a short-circuit switch, to reduce the discharge time, this configuration re- sulted in a significant decrease in flow contamination. Force tests in the Mach number range from 16-22 at stagnation temperatures from 3000-4000°K and stagnation pressures</p>	<p>1 Wind tunnels 2 Design 3 Growth 4 Hypervelocity I AFSC Program Area 750A, Project 8852, Task 88512 Contract AF 40(600)-800 S/A 24(61-73) III ARO, Inc., Arnold AF Sta, Tenn. IV J. A. van der Bliek V Available from OTS VI In ASTIA collection</p>
<p>from 10,000-20,000 psi were in good agreement with re- sults from other tunnels. An arc-chamber liner material study was carried out in the capacitance-driven Tunnel Hotshot 1. The materials tested included copper, boron nitride, graphite, tungsten, and chrome-plated copper. The heat losses through the arc-chamber walls of Hotshot 1, determined from runs at stagnation temperatures from 3000-9000°K, are presented, and their implications on hot- shot tunnel operation are discussed.</p>	<p>from 10,000-20,000 psi were in good agreement with re- sults from other tunnels. An arc-chamber liner material study was carried out in the capacitance-driven Tunnel Hotshot 1. The materials tested included copper, boron nitride, graphite, tungsten, and chrome-plated copper. The heat losses through the arc-chamber walls of Hotshot 1, determined from runs at stagnation temperatures from 3000-9000°K, are presented, and their implications on hot- shot tunnel operation are discussed.</p>	<p>from 10,000-20,000 psi were in good agreement with re- sults from other tunnels. An arc-chamber liner material study was carried out in the capacitance-driven Tunnel Hotshot 1. The materials tested included copper, boron nitride, graphite, tungsten, and chrome-plated copper. The heat losses through the arc-chamber walls of Hotshot 1, determined from runs at stagnation temperatures from 3000-9000°K, are presented, and their implications on hot- shot tunnel operation are discussed.</p>	<p>from 10,000-20,000 psi were in good agreement with re- sults from other tunnels. An arc-chamber liner material study was carried out in the capacitance-driven Tunnel Hotshot 1. The materials tested included copper, boron nitride, graphite, tungsten, and chrome-plated copper. The heat losses through the arc-chamber walls of Hotshot 1, determined from runs at stagnation temperatures from 3000-9000°K, are presented, and their implications on hot- shot tunnel operation are discussed.</p>